[eCoast, 2018:C1.1]

Wairoa WWTP Outfall: 3D Hydrodynamic Numerical Modelling

Prepared for

Wairoa District Council

eCoast
eTakutai

MOHIO - AUAHA - TAUTOKO
UNDERSTAND - INNOVATE - SUSTAIN

PO Box 151, Raglan 3225, New Zealand
Ph: +64 7 825 0087 | info@ecoast.co.nz | www.ecoast.co.nz

Wairoa WWTP Outfall: 3D Hydrodynamic Numerical Modelling

Report Status

Version	Date	Status	Approved by
V1	19 September 2018	Final Draft	STM
V2	14 October 2018	Rev 1	STM
V3	14 November 2018	Rev 2	STM
V4	24 November 2018	Rev 3	STM

It is the responsibility of the reader to verify the version number of this report.

Authors

Dougal Greer *MSc*

Shaw Mead *BSc, MSc (Hons), PhD*

Executive Summary

A combined field data collection and 3D hydrodynamic numerical modelling project for the Wairoa River and the Wairoa WWTP discharge was undertaken as part of the resource consent renewal process to better understand the dynamics of wastewater discharged into the estuarine and marine environments from the wastewater system. The field data campaign included the successful collection of current, salinity, sea level and bathymetry data in the river mouth and the lower reaches of the river. These data were used to development the nearfield model grid/domain and calibrate and validate the 3D hydrodynamic numerical model. It should be noted that the morphology of the river mouth regularly changes over time and this will have some influence over hydrodynamics of the area which will in turn influence the pattern of dilution of the outfall.

The model calibrated reasonably well against measured data in this hydrodynamically complex location, and replicated the important processes and degree of stratification identified in the measured data. This provides confidence in the results of the various modelled discharge and overflow scenarios modelled.

The model was used to simulate a representative period of the operation of the outfall and to show percentile outfall dilution maps in the river mouth which can be used to describe the spatial variability in influence of the outfall. An additional simulation was run to investigate the effects of a 3-year ARI rainfall event that resulted in a wastewater spill at 3 locations (this event in March 2012 was the only event for which flow data is available for model simulation). Dilution maps indicate rapid mixing of the plume in the fast-flowing river associated with the rain event.

The model was next used to explore the dilution of the wastewater spatially throughout the estuary for 10 scenarios with different configurations of outfall flow, timing and river flow to represent potential future outfall discharge regimes.

The model was not used to model specific contaminants (such as bacteria, nutrients, viruses and sediment) and specific concentrations of contaminants. However, the dilution maps and transect graphs developed from the model outputs can be used to provide conservative estimates of pollutant concentrations from assumed pollutant concentration at the outfall or overflow and at varying distances from the outfall location. As no pollutant concentrations have been used no attenuation or assessments of discharge effects on river water quality have been included in the modelling.

The model was also used to show the spatial variability in bed shear stress highlighting areas of active erosion and areas of expected deposition. These results indicate that future

ecological and sediment composition monitoring should include the western arm of the lower estuary, where outfall water is often retained and shear stress is low.

Contents

Figures

Tables

1 Overview

The resource consent for the Wairoa River Waste Water Treatment Plant (WWTP) is due to expire in May 2019. As part of the renewal process this study is being undertaken to better understand the dynamics of wastewater discharged into the marine environment from the wastewater system. The study was undertaken in two parts: the first was a field data collection programme within the Wairoa River (which included an ecological assessment and sediment analysis (Mead *et al*., 2018)) and the second was a numerical modelling study to understand the dispersion of the wastewater plume through time and under the influence of a number of interacting forces.

1.1 Study Site Review

The outfall for the Wairoa WWTP is located on the western bank of the Wairoa River near the river mouth (see Figure 1.1) where it is approximately 320 m wide. The outfall is consented to release on the outgoing tide between the hours of 6 pm and 6 am.

The river mouth is a tidal river estuary with a very mobile mouth. Figure 1.2 shows the movement of the river mouth on three occasions in 2006, 2011 and 2012 showing lateral movement of the mouth of at least 800 m through the three images. The mouth also occasionally closes in response to marine conditions turning the estuary temporarily into a lagoon. It is occasionally reopened by the Hawkes Bay Regional Council (HBRC)using a digger[1]. During the bathymetry survey, the mouth configuration was closest to 2012 in Figure 1.2, although there was a small island in the centre of the main channel close to the estuary mouth. Just inside the estuary mouth, the river features two intertidal regions running approximately east and west, away from the principle river channel (Figure 1.2).

A record of wind from 2012 to 2018 (Figure 1.3) taken from the Wairoa Aero Automatic Weather Station (AWS) show prevailing winds form the NW rarely exceeding 10 ms^{-1}. The tide on the open coast is semi-diurnal with a spring tidal range of approximately 1.9 m and a neap tidal range of approximately 1.2 m.

[1] https://www.lawa.org.nz/explore-data/hawkes-bay-region/river-quality/wairoa-river/

Figure 1.1. Wairoa River mouth and relevant landmarks.

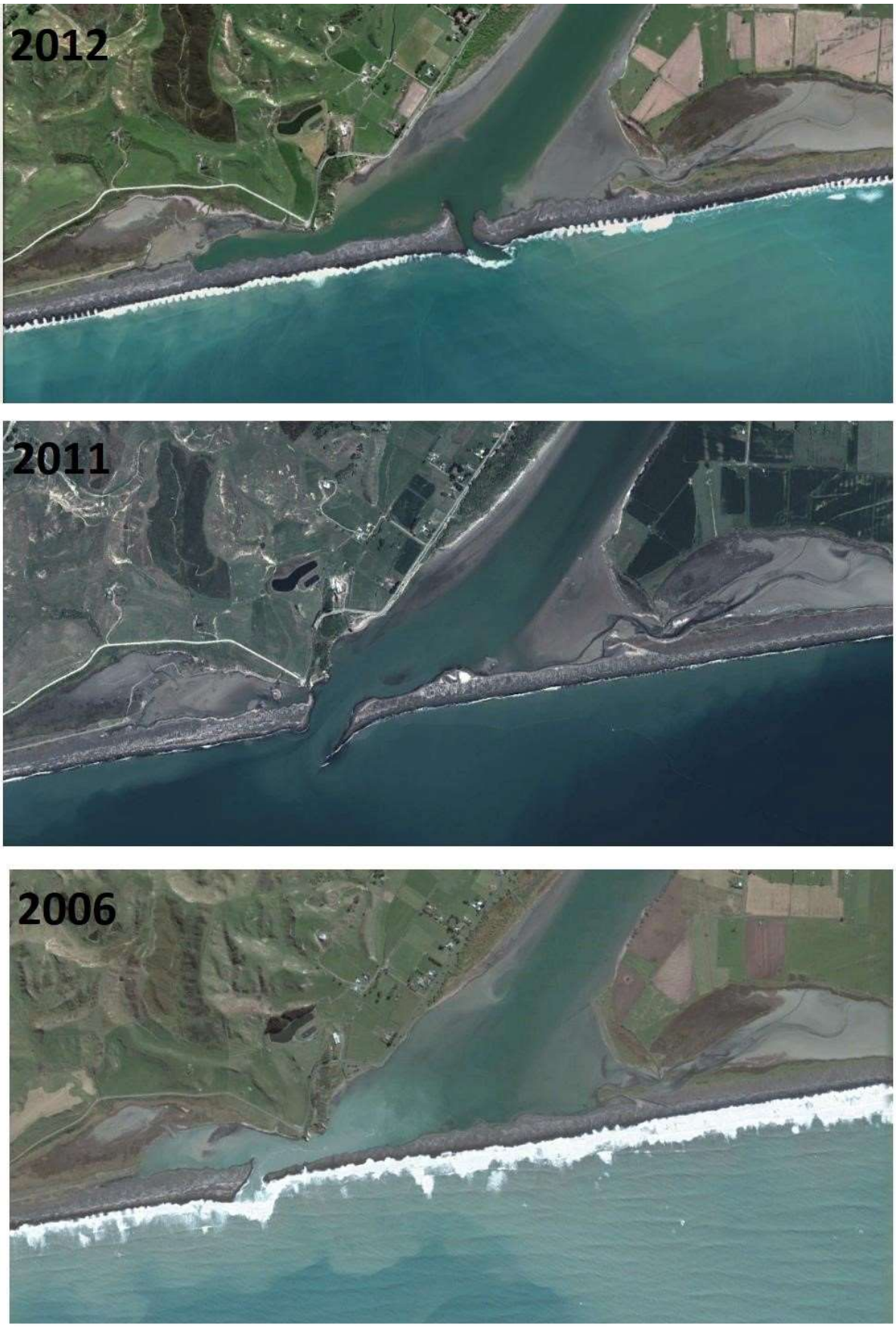

Figure 1.2. a series of aerial images illustrating the mobile morphology around the Wairoa River estuary mouth (source: Google Earth).

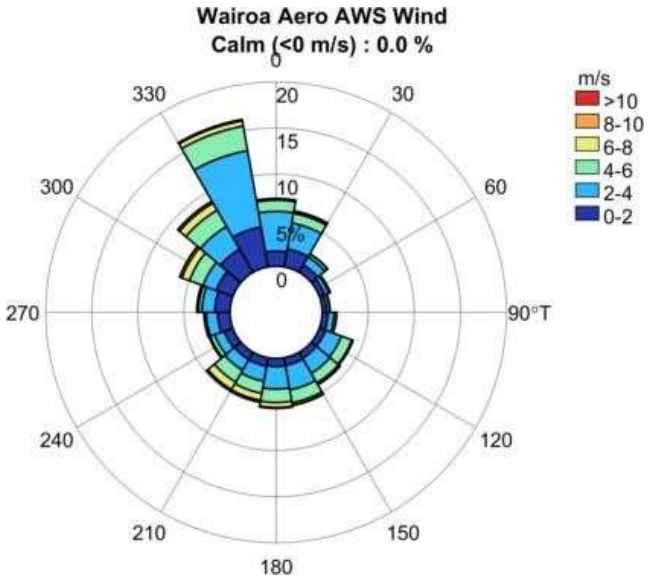

Figure 1.3. Wind rose created from Wairoa Aero AWS summarising wind data from 2012 until 2018.

2 Fieldwork

Fieldwork was undertaken on 18-20th April 2018 in the lower Wairoa River, and the wave/current/water level instrument (a Nortek Aquadopp) was retrieved from its location approximately 150 m southeast of the outfall on 19th May 2018. The fieldwork programme included:

- Bathymetry survey of the lower part of the Wairoa River (Figure 2.1);
- Sediment and ecological sampling at 10 sites in the estuary, including distant upriver sites as controls (Figure 2.2);
- Deployment of a wave/current/water level meter with a salinity meter ~150 m southeast of the outfall in the main estuary channel, and a salinity meter close to the estuary entrance (Figure 2.2), and;
- A salinity transect (using a YSI multi-meter (maximum depth 4 m)) down the main channel past the outfall during an outgoing tide (Figure 2.3).

2.1 Field Work Methodology

Since the only publicly available bathymetry data for the river and estuary is of the relatively coarse nautical chart of the Hawke's Bay (NZ5601), a bathymetry survey was undertaken in order to develop modelling grids/domains. Run-lines were programmed into the survey system and used to guide the survey path (Figure 2.1). The survey used standard techniques with a sounder and GPS. A LOWRANCE LMS-525 single-beam echo sounder at 200 KHz working in conjunction with a GPS unit, recorded the depth and position data in real-time to a palmtop computer.

A lead-line test was undertaken to test the sonar and quantify the vertical accuracy of the measurements. The sonar has a temperature sensor for automatic temperature compensation for speed of sound through water, thus this effect is accounted for in the survey. The lead-line depth was compared to the sounder readout on the screen from 2 m to 8 m deep (off of the Ski Club Boat Ramp – Figure 2.2). The tests included compensation for the depth of the sounder which was measured at 0.4 m below the water surface. The results of the calibration tests showed that the sounder was within the instruments specifications (i.e. +/- 0.1 m) at these depth ranges.

The data was corrected to MSL at the instrument and the river level fall, and further data (WDC river bathymetry transects, GEBCO offshore data, digitised chart data and digitised satellite images) to develop the nearfield model grid (Figure 2.4 and Figure 3.1).

Figure 2.1. The bathymetry survey path of the lower Wairoa River and sampling and deployment locations. Note, there were no bathymetric measurements in the entrance channel itself due to health and safety concerns around using the survey vessel in the turbulent high flow conditions in the channel.

Figure 2.2. Locations of sampling and instrument deployment sites.

Figure 2.3. Salinity transect sampling locations.

2.2 Field Data Results

2.2.1 Bathymetry Survey

The compile bathymetry data was converted using Quickin in order to develop the nearfield curvilinear modelling grid (Figure 2.4).

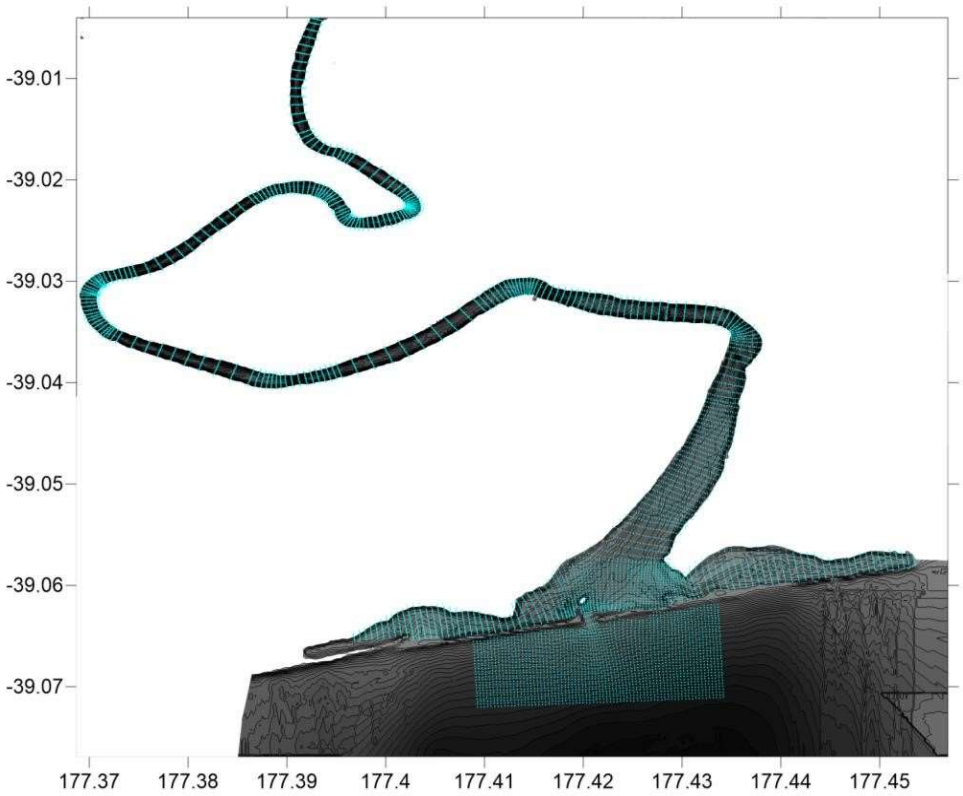

Figure 2.4. Final compiled bathymetry data for the generation of the curvilinear model grid (Figure 3.1).

2.2.2 Instrument Deployments

Figure 2.5 presents the water level measured by the Aquadopp close to the outfall (Figure 2.2). The time series data clearly shows the effect of rainfall/increased river flow rates. These data were used for model calibration in the following Section.

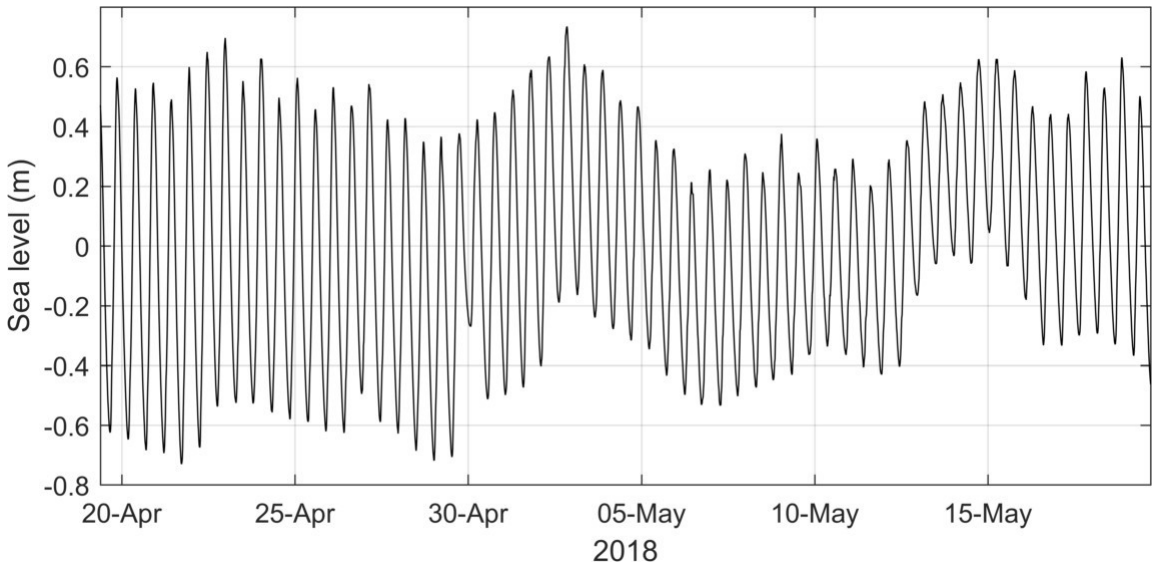

Figure 2.5. Sea level timeseries recorded by the current meter.

Figure 2.6 presents the current speed and direction recorded by the Aquadopp close to the outfall (Figure 2.2). The tidally-driven directional reversals along the NE-SW axis of the estuary channel location is very clear in the data, while the effects of rainfall/increased river flow rates seen in the water level data (Figure 2.5) are also reflected in the current speeds. Current speeds exceeded 0.5 m/s during the high flow event in early May (Figure 2.6). These data were used for model calibration in the following section.

The effects of the tidal reversal and rainfall/increased river flow rates are also clearly evident, with lower salinity occurring during periods of higher current speeds (Figure 2.7 and Figure 2.6). These data were also used for model calibration in the following Section.

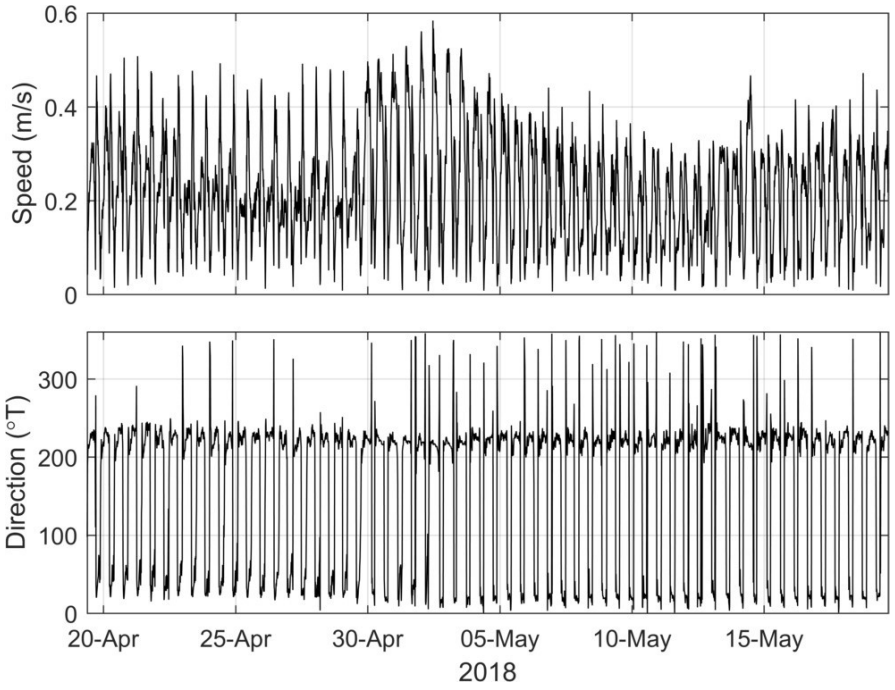

Figure 2.6. Current speed (upper panel) and direction (lower panel) recorded by the current meter.

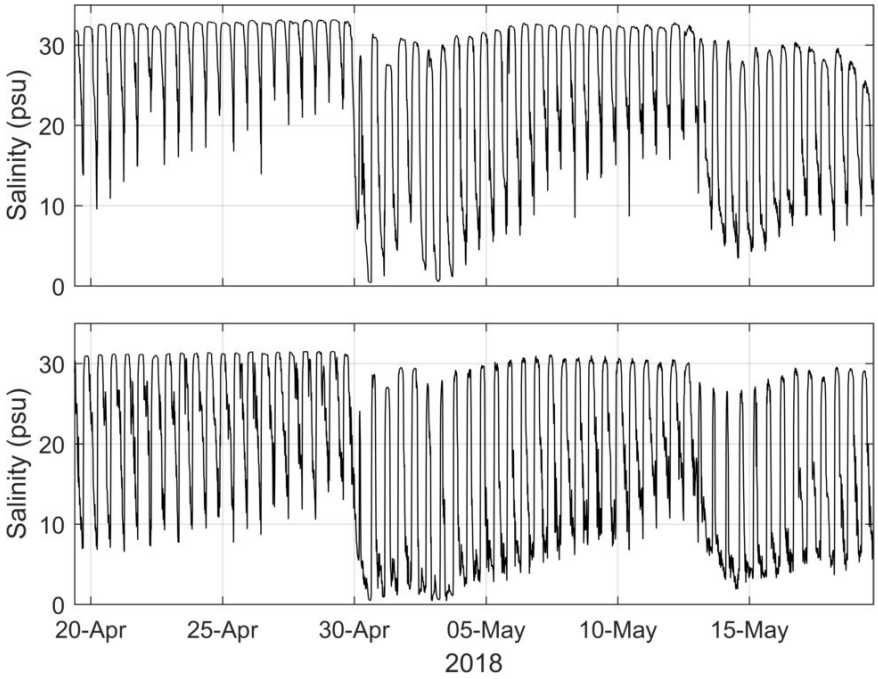

Figure 2.7. Salinity recorded at the Aquadopp location (upper panel) and at the Entrance location (lower panel).

2.2.3 Salinity Transect

The salinity transect was measured at the end of the deployment period, prior to the retrieval of the instruments. These data were collected in order to validate stratification in the 3D model, and the results are presented in Table 2.1 below.

Table 2.1. The results of the salinity transect – locations are also presented in Figure 2.3.

Site	Lat	Long	Surface (ppt)	1.2 m deep (ppt)	Bottom (ppt)
809	-39.05583	177.425837	2.3	13.9	30.4
810	-39.05659	177.425415	2.6	15	30.5
811	-39.057303	177.42442	2.75	13.4	26.9
812	-39.058401	177.423079	3.4	9.1	19.9
814	-39.059811	177.421056	3.4	7.4	20
815	-39.060985	177.419346	3	5.4	12.4
816	-39.061803	177.420297	2.7	6	10.3

2.2.4 Ecological and Sediment Sampling

The results of the ecological and sediment sampling are detailed in the associated report "Assessment of effects of Wairoa District Council's intertidal sewage discharge on benthic sediment characteristics and ecology – Wairoa Estuary" (Mead *et al*., 2018). Sampling locations are shown in Figure 2.2

3 Model Development and Calibration

The model developed for this study is a 3D hydrodynamic model with 5 sigma layers divided as follows: 10%, 25%, 30%, 25% and 10%. The model was forced with wind, tides, river flow and the wastewater outfall and also included salinity.

3.1 Model Overview

For this project we use the Delft Flow module from the Delft3D Model Suite which is an industry standard for hydrodynamic numerical modelling. Delft3D is an open source project meaning that improvements in the software come from a large-scale collaborative effort including internal developers as well as from a broad base of users worldwide.

The modelling setup used a system of nested model grids using a nesting process known as Domain Decomposition (DD). Standard nesting procedures use a coarse model run over a large model domain, and nested boundary conditions are extracted from this to run higher resolution models covering a smaller area contained within the domain of the coarse grid. DD is a dynamically coupled nesting system whereby the coarser and finer grids are run simultaneously, and information is passed between the domains (Deltares, 2013). This means that trace substances can pass seamlessly between the two grids in a way that is not possible using standard nesting. Furthermore, information pertaining to other hydrodynamic processes is not lost between domains in the nesting process as it is using standard nesting.

Results from the modelling are shown as dilution by ambient water and in most cases, the spatial plots show up to 1000-fold dilution.

3.2 Bathymetry Grids

The model was setup using a series of 4 nested grids with increasing resolution closer to the outfall. The three outer grids were rectilinear with a curvilinear approach being used in the highest resolution nest to represent the river estuary. As noted previously the morphology of the river, particularly near the mouth, is very dynamic. Morphological changes in the model domain would be difficult to incorporate into a numerical model, so the model bathymetry was therefore represented as a stable bathymetry based on measured data (Section 2 above).

The bathymetry grids were developed using depth data from LINZ hydrographic charts for the offshore grids in conjunction with the bathymetry survey data. The highest resolution grid also made use of the bathymetry data from the field work, as well as river transects from the HBRC and extended approximately 15 km upstream as far as the railway bridge. The point cloud

data was converted to gridded depths using krigging for the 3 outer grids and using the Delft3D package Quickin for the curvilinear grid. Since there were no measurements for the entrance channel depth (it could not be surveyed due to safety issues in this very fast flowing and wave effected area), this had to be treated as a calibration parameter. The final bathymetry grids are shown in Figure 3.1.

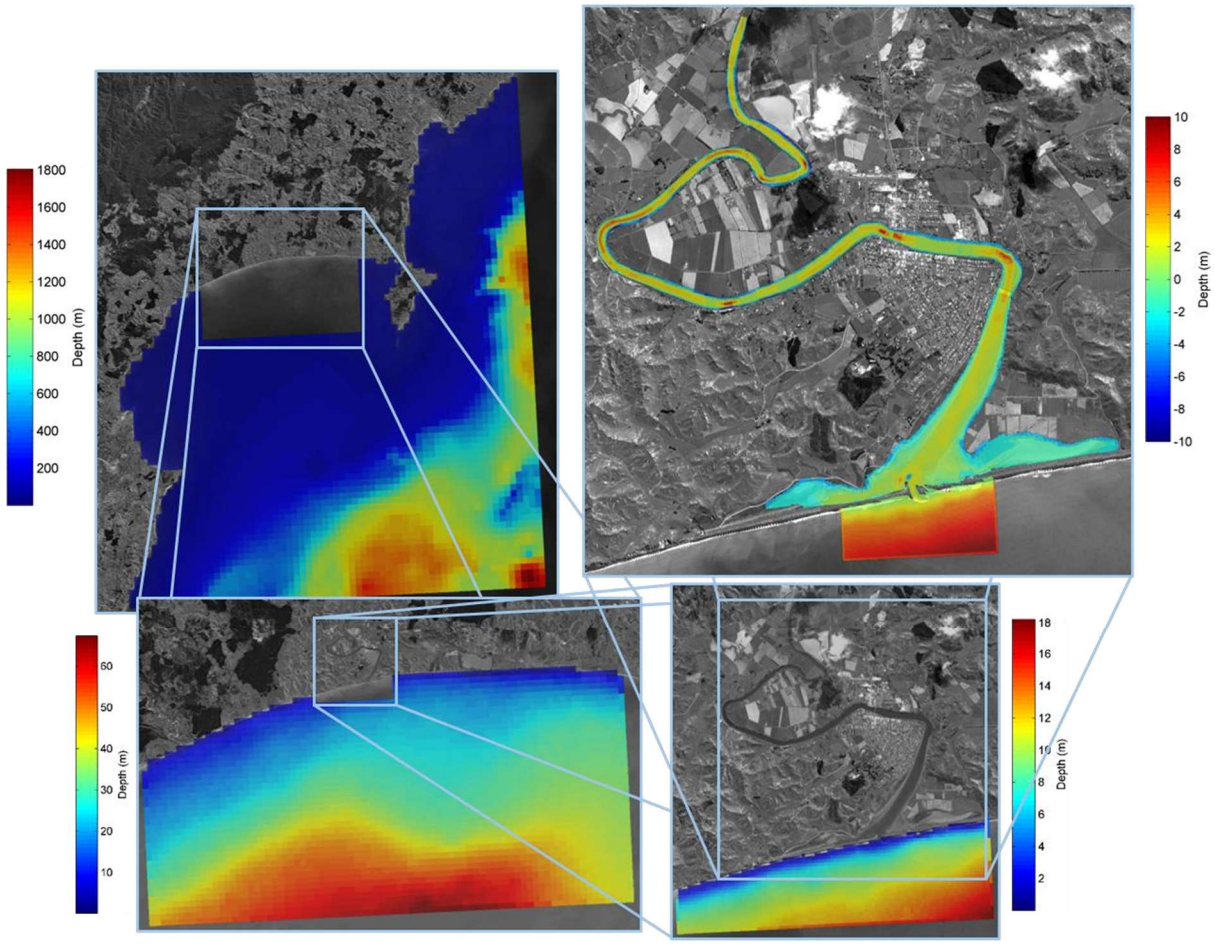

Figure 3.1. Nested bathymetry grids used in the hydrodynamic model.

3.3 Boundary Conditions

Tidal boundary conditions on the open ocean boundaries of the model were extracted from the TPXO wave atlas (Egbert and Erofeeva, 2002). This model was developed by the Oregon State University, who created a global model of ocean tides which uses along track averaged altimeter data from the TOPEX/Poseidon and Jason satellites since 2002. The methodology applied in the global tide models has been refined to create regional models at higher resolution modelling here. For this project, we used the Pacific Ocean model with a resolution of 1/12 degree. The model provided the 11 most influential constituents, as well as two long period

(Mf, Mm) harmonic constituents. Each constituent is a sinusoid which represents the gravitational influence of a particular aspect of a planetary body or of several bodies. Each sinusoid was described in the model by a phase and amplitude of the sinusoid and these were extracted at regular intervals along the model boundary.

Wind boundary conditions in the model were created using a long-term hourly wind record from the Wairoa Aero AWS extracted from NIWA's Cliflo[2] website.

The upstream boundary (to the north) was represented using hourly river stage data recorded at the railway bridge and provided by HBRC. This boundary was set to 0 psu and provided the river flow into the model domain.

The wastewater outfall was created using recorded data describing the daily discharge and valve opening times (recorded every 15 minutes). The outfall was represented as a single cell in the intertidal zone using a 'walking' release meaning that if the release cell was dry, the model discharges into the nearest wet cell. The wastewater was discharged into the top layer of the model minimising mixing of the plume with lower layers and providing a conservative estimate of plume dilution. The wastewater was also represented by a conservative tracer in the model so that it could be discerned from the freshwater introduced from river flow.

3.4 Model Calibration

The model calibration simulation was run for the duration of the instrument deployments with a 2-day lead in time from 17 April 2018 until 20 May 2018.

The dynamics of the model were found to be sensitive to model parameters due to the complex interaction of the river flow with saline water entering the estuary through the narrow entrance. The model was calibrated by comparing modelled sea level, currents and salinity with measured values obtained during the field data collection period (Section 2 above). Boundary conditions for the calibration period are shown in Figure 3.2. The period covered several spring neap cycles and captured a strong wind event (8 m s^{-1} from the SW) between 30 April and 5 May 2018. During this period, river levels were elevated, and outfall flows were high. There was a small break in the wind record between 21 April and 23 April. This gap was filled using linear interpolation.

Comparing the wind record during the calibration period with the wind record full 6-year wind record from the Wairoa Aero AWS (Figure 3.3) shows it to be reasonably representative of the full record. Additionally, a comparison of the outfall flow record during the calibration period

[2] https://cliflo.niwa.co.nz/

with the full record of flows (Figure 3.4) shows the calibration period flows to be higher than usual and to contain periods of high flow.

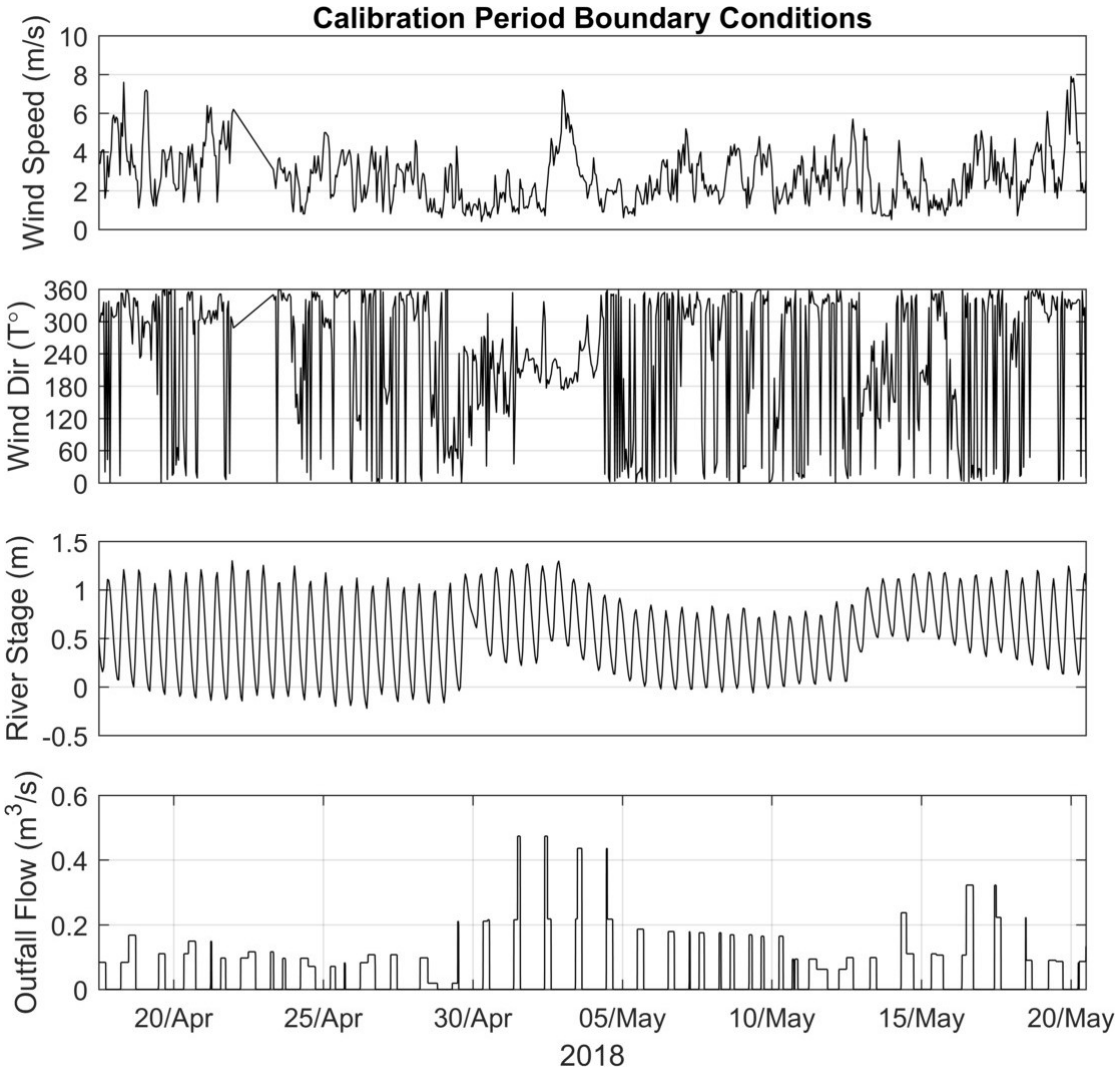

Figure 3.2. Boundary conditions used to drive the model for the calibration period.

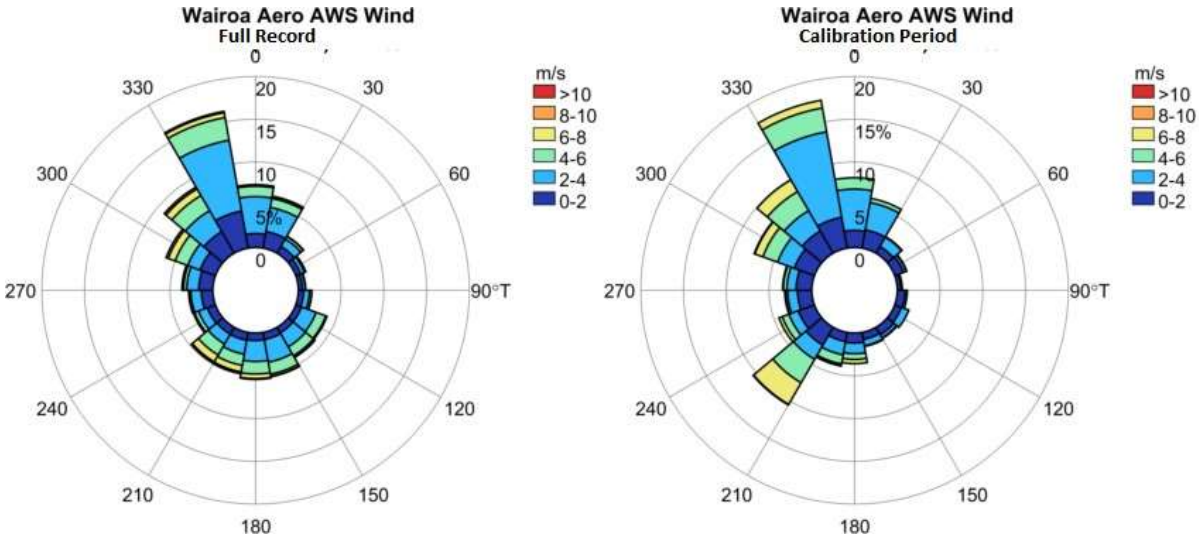

Figure 3.3. Wind roses from the full record of wind recorded at the Wairoa Aero AWS (left) compared with wind recorded during the calibration period.

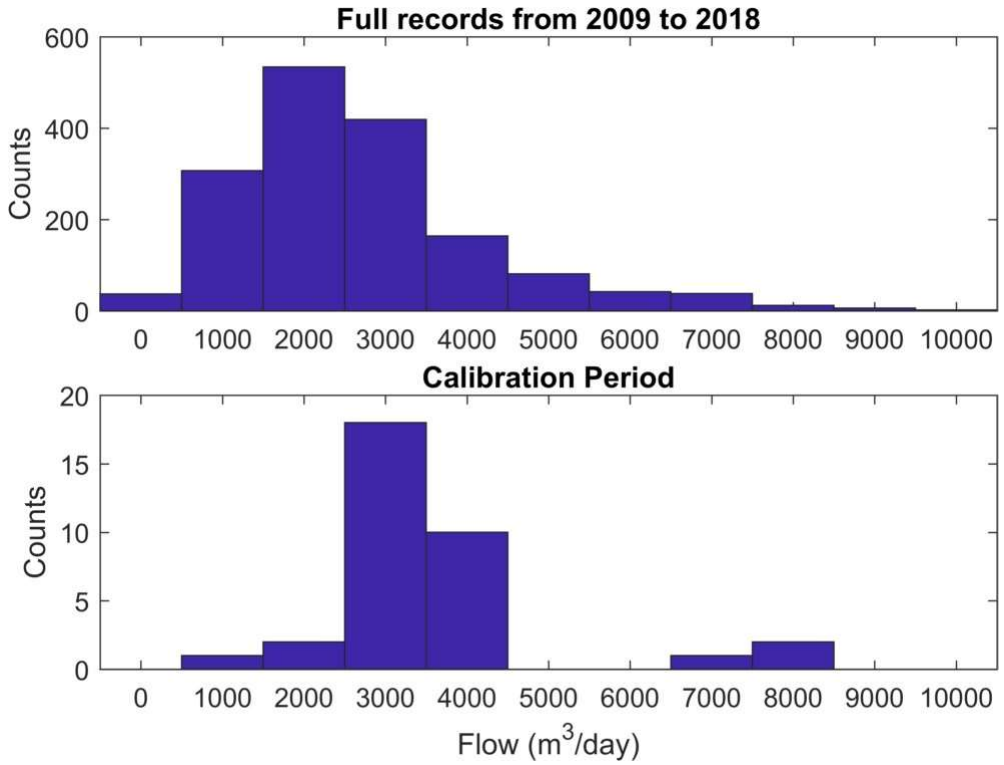

Figure 3.4. The full record of daily flow from the wastewater outfall (upper panel) compared with the daily flow during the calibration period (lower panel).

The model was run multiple times to find an optimal set of model parameters; the location of the outfall and the variety of physical parameters (e.g. freshwater, saltwater, a narrow entrance channel, large intertidal areas in the estuary, etc.) result in a very complex area to model. Model parameters that were explored included horizontal eddy viscosity, horizontal eddy diffusivity, entrance channel depth, river stage offset and friction. The model performance was

found not to be very sensitive to the addition of wind effects. The final model parameters are shown in Table 3.1.

Comparisons were undertaken between measured and modelled sea level, currents and salinity from the field data collection (Section 2). The model reproduced sea level reasonably well (Figure 3.5) and captured the tidal variability throughout the run. Unlike on the open coast, the tidal signal in a river dominated estuary becomes distorted during high flow conditions (e.g. between 30 April and 5 May). The currents are highly asymmetrical and reasonably well reproduced by the model (Figure 3.6), although during high flow the model does not replicate the maximum currents speeds measured by the current meter (this means results are conservative for high flow scenarios).

Salinity is the most challenging signal to reproduce in the model since, in this environment, it is expected to vary markedly in both the vertical and horizontal directions. Salinity was recorded in two locations for 4 weeks (Section 2.1) and was also recorded through a series of transects recorded at the end of the deployment period/model run. The model reproduced the measured salinity record reasonably well (Figure 3.7), although between 5 and 10 May the variability in the measured signal was not replicated in the model at the entrance location. Counterintuitively, the measured signal at the entrance location showed consistently lower salinity on the ebb tides than the Aquadopp location further upstream.

As discussed previously, the measured transects showed significant stratification through the water column but contrary to what would be expected they showed consistently lower salinity with increased proximity to the estuary mouth. Comparison with the transects extracted from the model at the same time (Figure 3.8) shows that this is not replicated by the model. However, the process by which this occurs is replicated by the model at other times and this is illustrated by a series of sequential plots showing salinity changing through space and time in Figure 3.9. Freshwater from the river gets trapped in the western arm of the river mouth as the tide changes from outgoing to incoming and the inflowing saline marine water bypasses this arm as it intrudes into the river. This gives rise to a decrease in surface salinity moving from the outfall in a downstream direction towards the western arm. This effect may be further compounded by small freshwater sources entering the river from the eastern and western arms of the river mouth. Further comparison of the measured transects with modelled transects several hours before the measured transects were undertaken shows that the degree of measured stratification is well represented in the model more broadly.

In summary, even though this is a very complex area to model, the model calibration has provided a reasonable degree of confidence for undertaking discharge scenario modelling.

Table 3.1. Model Parameters derived during the calibration process.

Model Parameter	Value Used
Horizontal eddy Viscosity	20 ms^2
Horizontal eddy Diffusivity	20 ms^2
Friction (Chezy)	80
Channel Depth	1.75 m
River stage offset	-0.25 m

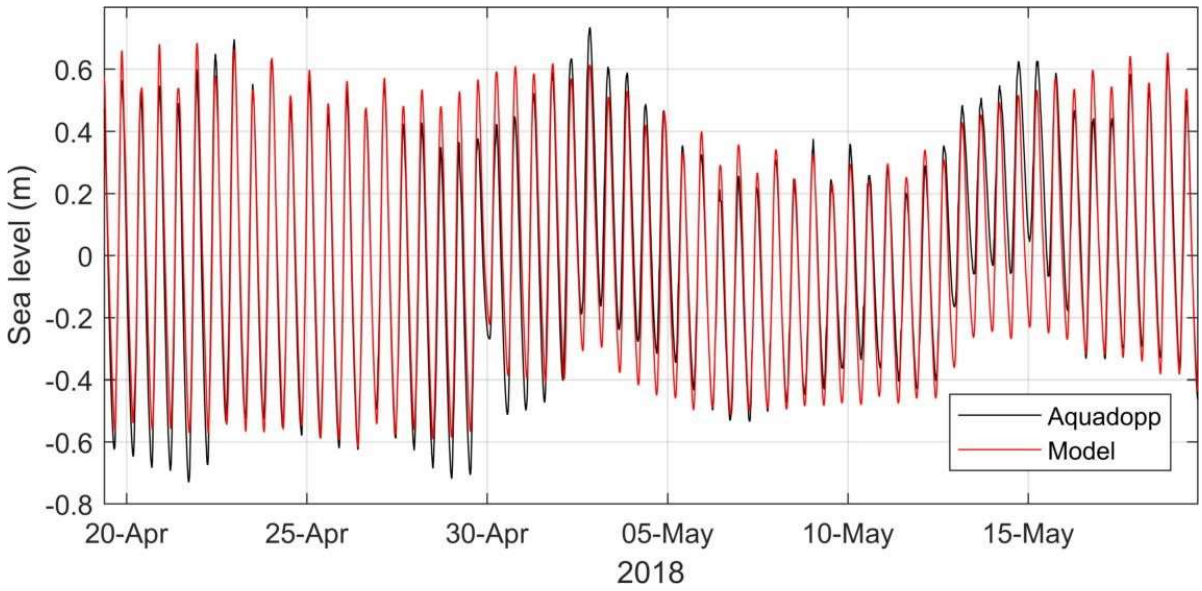

Figure 3.5. Comparison between measured and modelled sea level at the Aquadopp location.

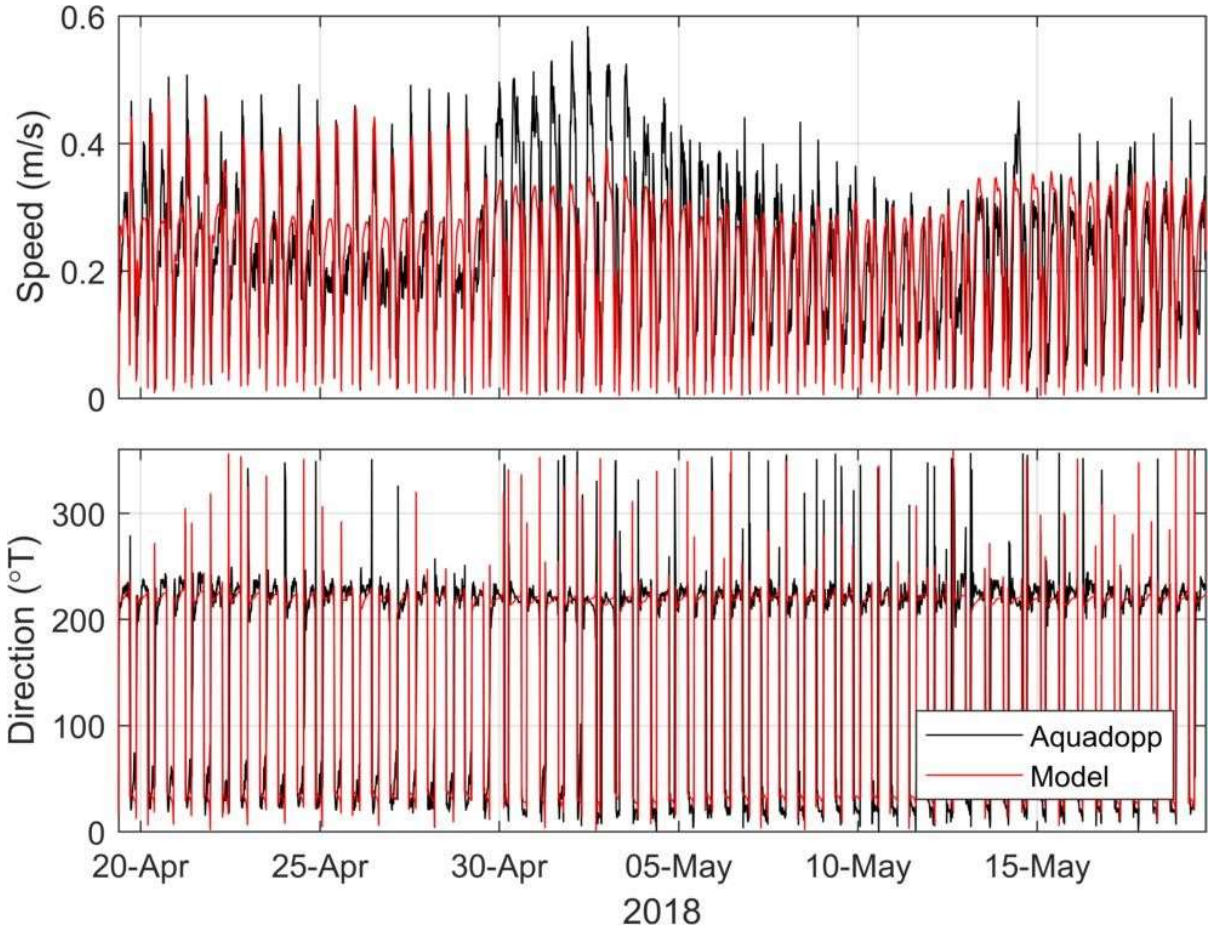

Figure 3.6. Comparison between measured and modelled current speed (upper panel) and direction (lower panel) at the Aquadopp location.

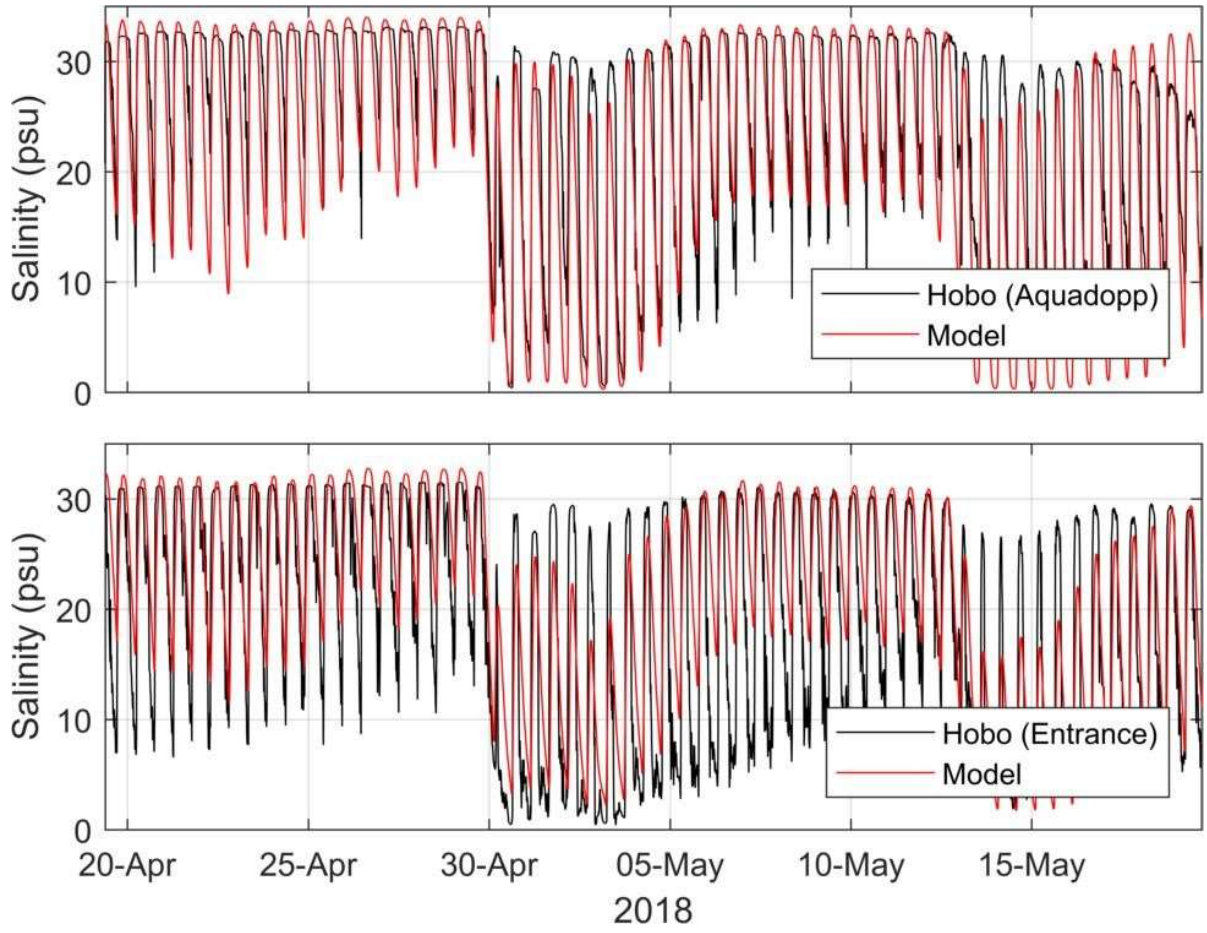

Figure 3.7. Comparison between measured and modelled salinity at the Aquadopp location (upper panel) and the Entrance location (lower panel).

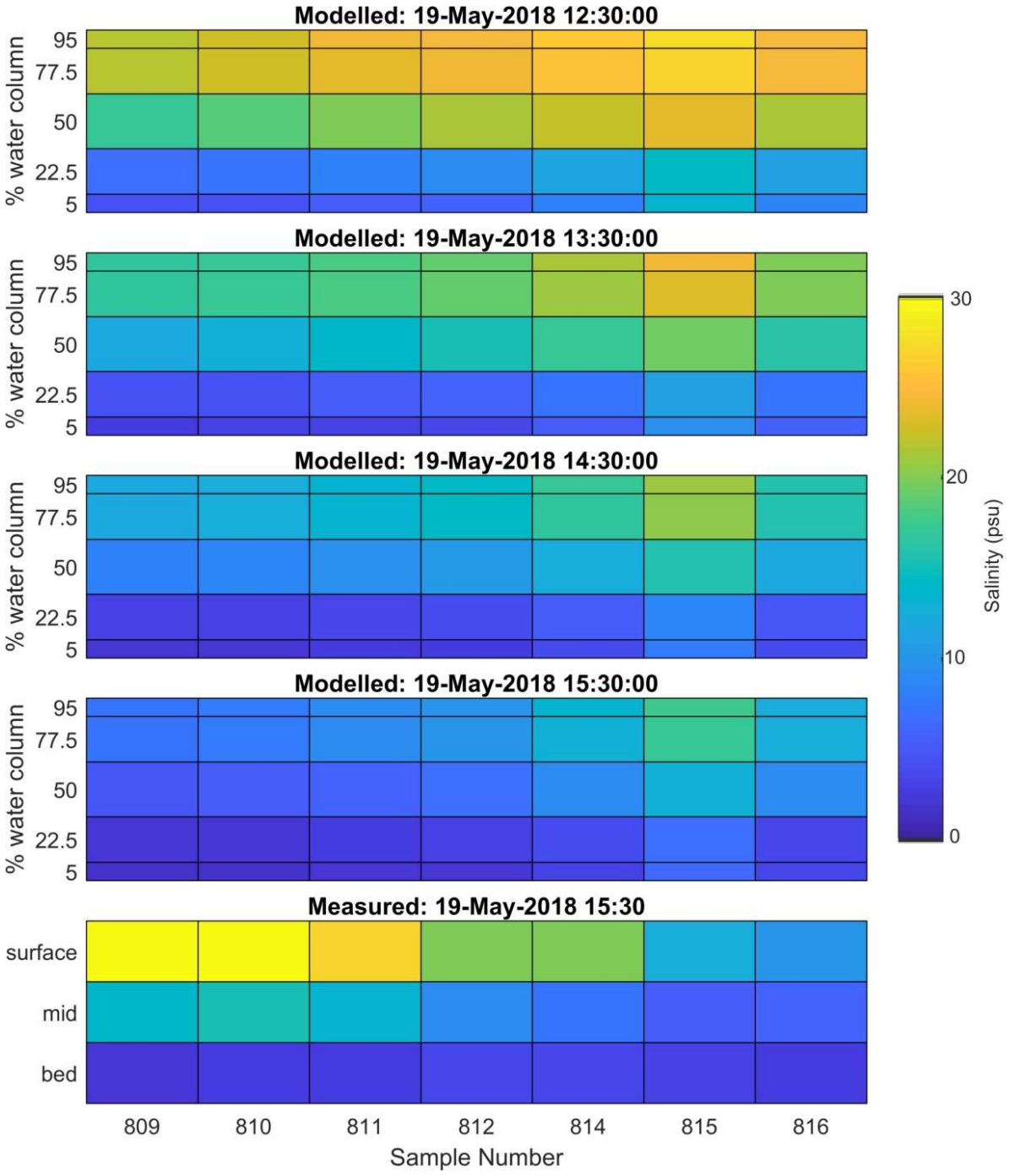

Figure 3.8. Modelled salinity transects from 4 different model times (upper four panels) and measured transect (lower panel).

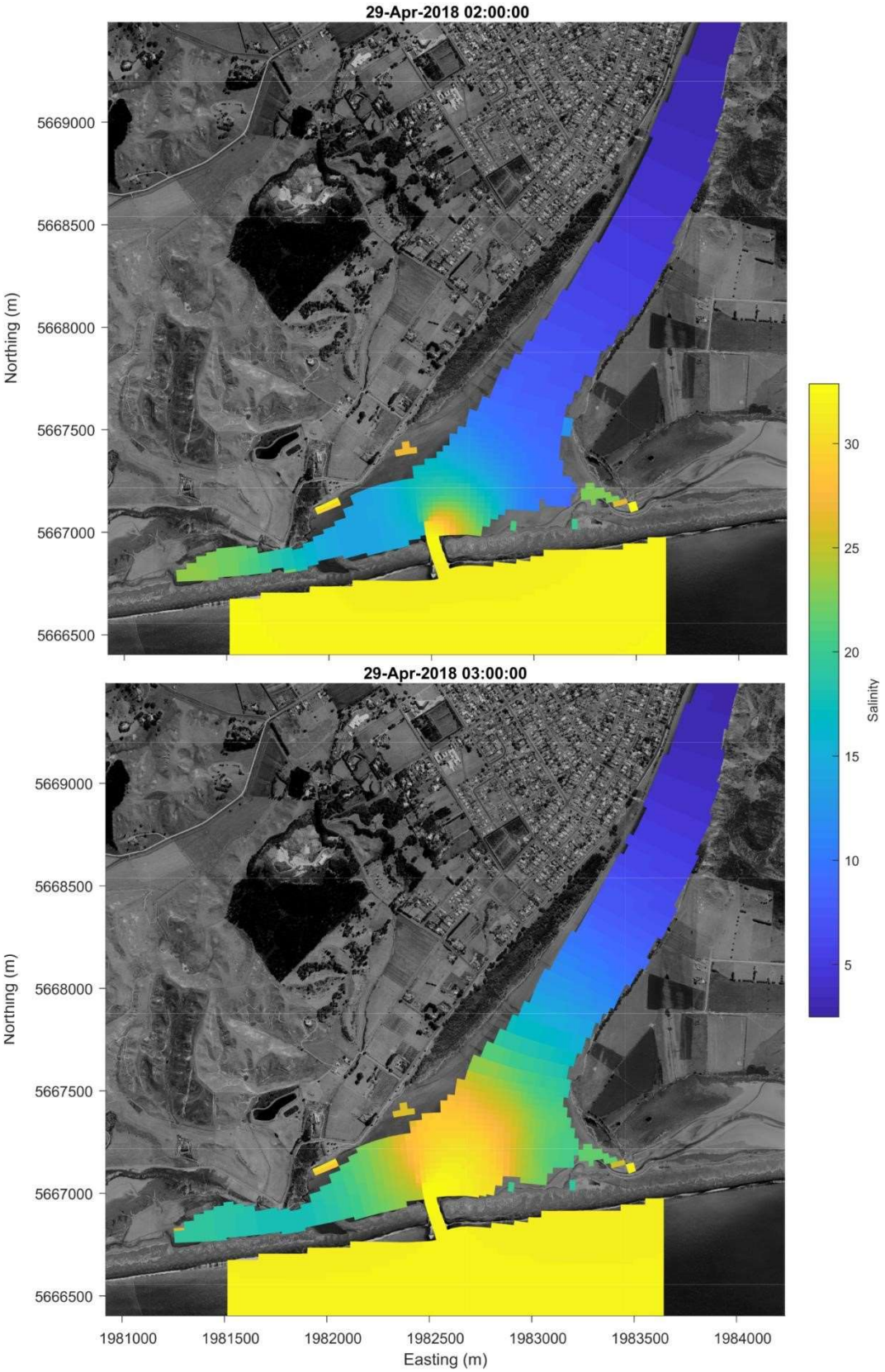

Figure 3.9. Modelled surface layer salinity over two timesteps illustrating how fresh water becomes trapped in the western arm of the entrance as the tide changes from outgoing to incoming tide.

3.5 Outfall Dilution

As discussed in Section 3.4 wind and flow conditions during the calibration period were broadly representative of the longer-term record erring on the side of being conservative. For this reason, the calibration model run was used to characterise the behaviour of the hydrodynamics and plume over time. All of the results shown in this section show the surface layer of the model as this is where the outfall water, which is released into the surface layer in the model, is most concentrated (lower salinity means less dense water, and so it floats to the surface).

Peak flood and ebb surface currents are shown in Figure 3.10 and illustrate the fast (3 m s^{-1}) currents through the entrance which would be expected to contribute to the highly mobile morphodynamics of the river mouth. Ebb tide currents are strengthened by the river flow and are stronger than flood tide currents. Vector averaged currents (Figure 3.11) show the seaward moving residual currents.

The conservative tracer released in the model was used to understand the mixing of the plume with distance from the outfall. It should be noted that in outfall release cell, is approximately 25 m by 25 m and in this area the mixing of the outfall water with ambient water should be treated with caution since, in the model, the outfall water was fully mixed within the top layer of that cell. Plume dilution (d) was calculated from salinity in the model as follows:

$$d = \frac{35}{35 - s}$$

where 35 (ppt) is the background salinity and s is the salinity in the model. Dilution was calculated throughout the model domain for all timesteps after the 2-day spin up period and percentiles of dilution were calculated at each model cell. 80th, 90th, 95th and 99th percentile maps are shown in Figure 3.12 and Figure 3.13 and illustrate the dominant movement of the outfall plume towards the river mouth and into the western arm of the mouth. The plume dilutes rapidly with distance from the outfall as it is transported away from the outfall by river flow combined with ebb tidal currents.

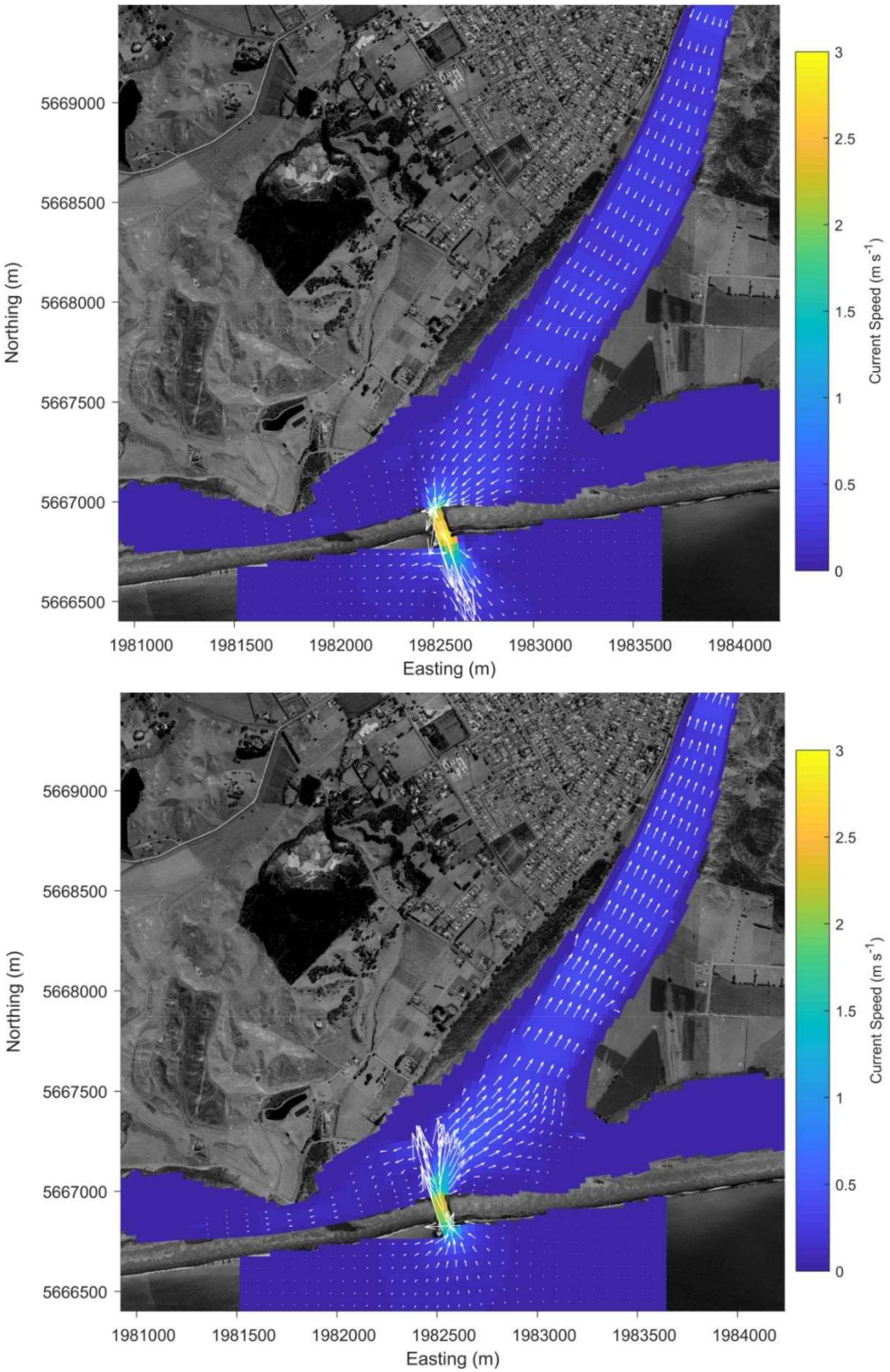

Figure 3.10. Surface layer peak ebb (upper panel) and flood tidal currents at the study site.

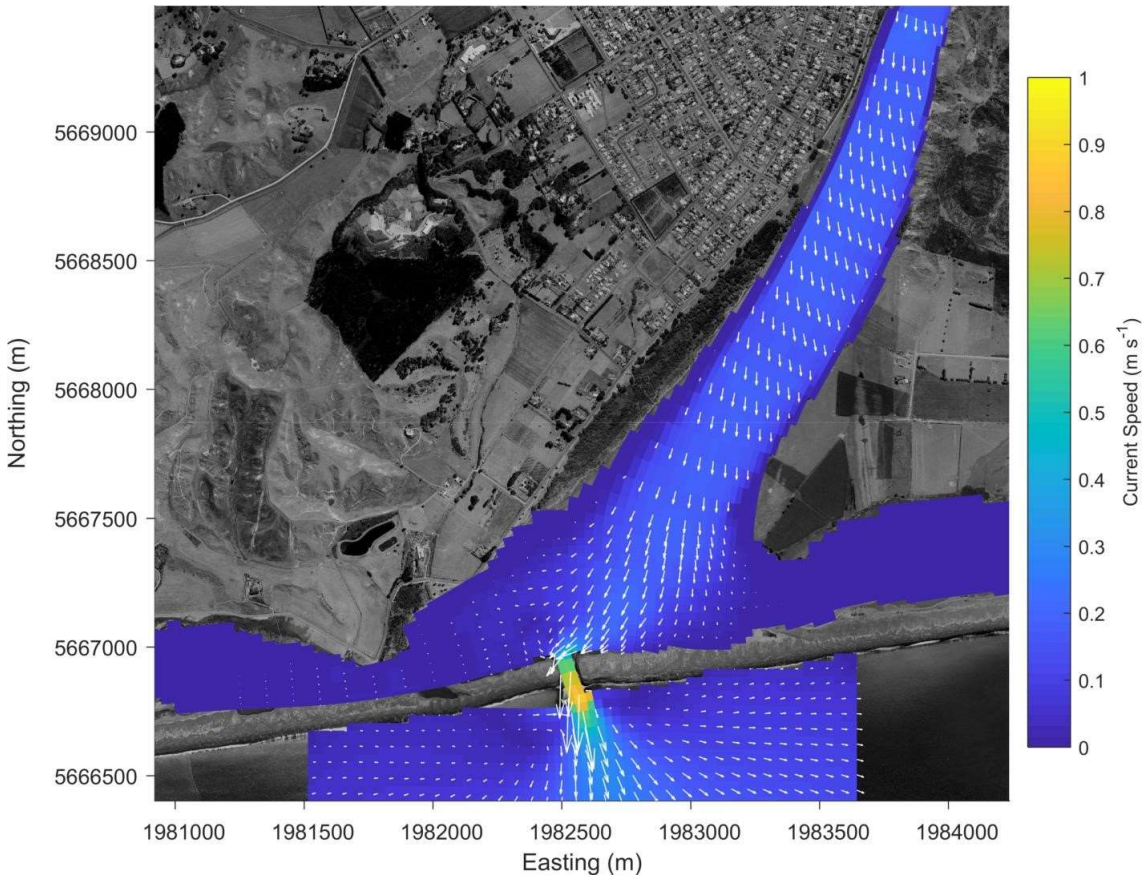

Figure 3.11. Residual currents for the calibration period.

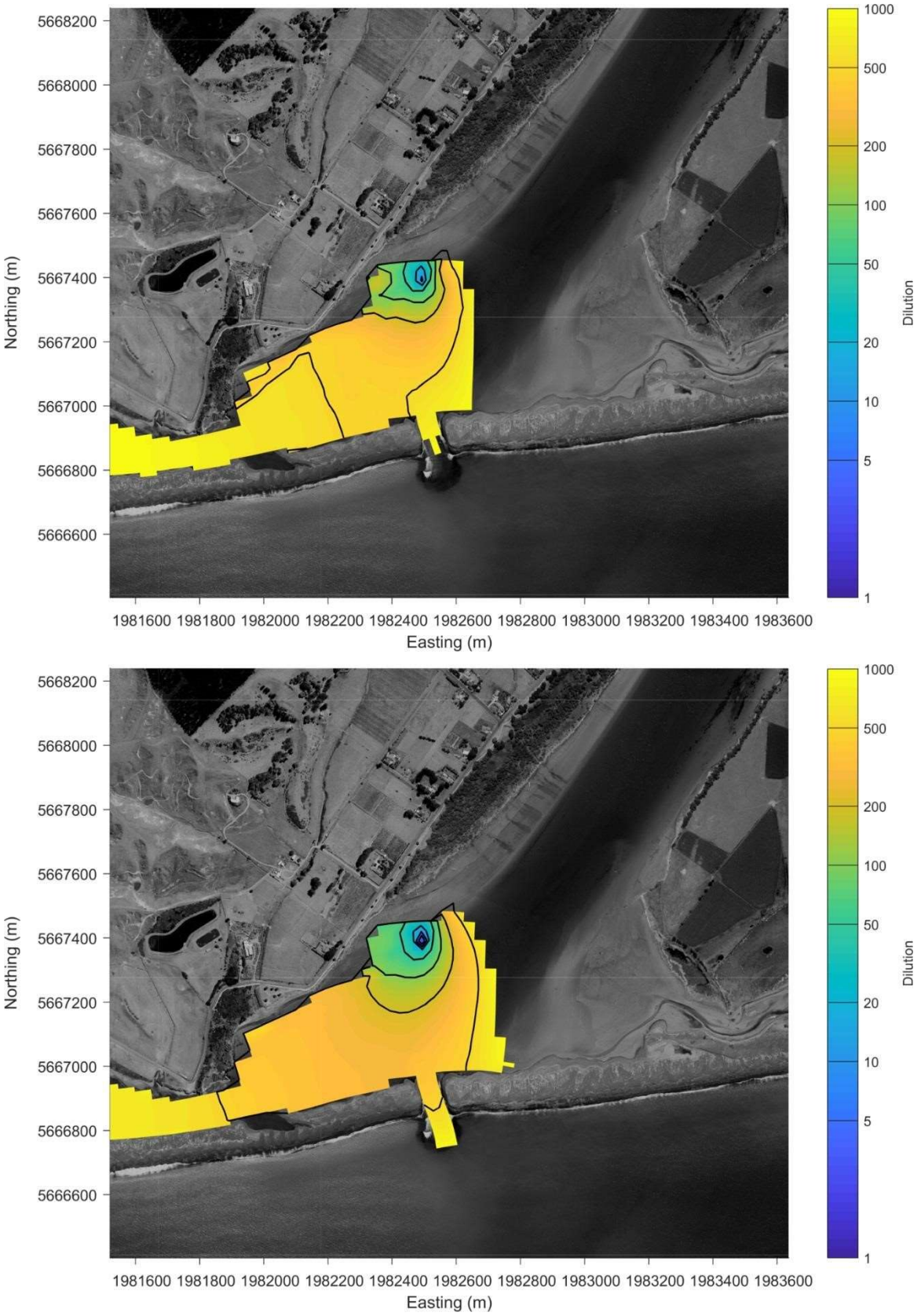

Figure 3.12. Dilution of the outfall for the calibration period. 80th (upper panel) and 90th (lower panel) percentiles.

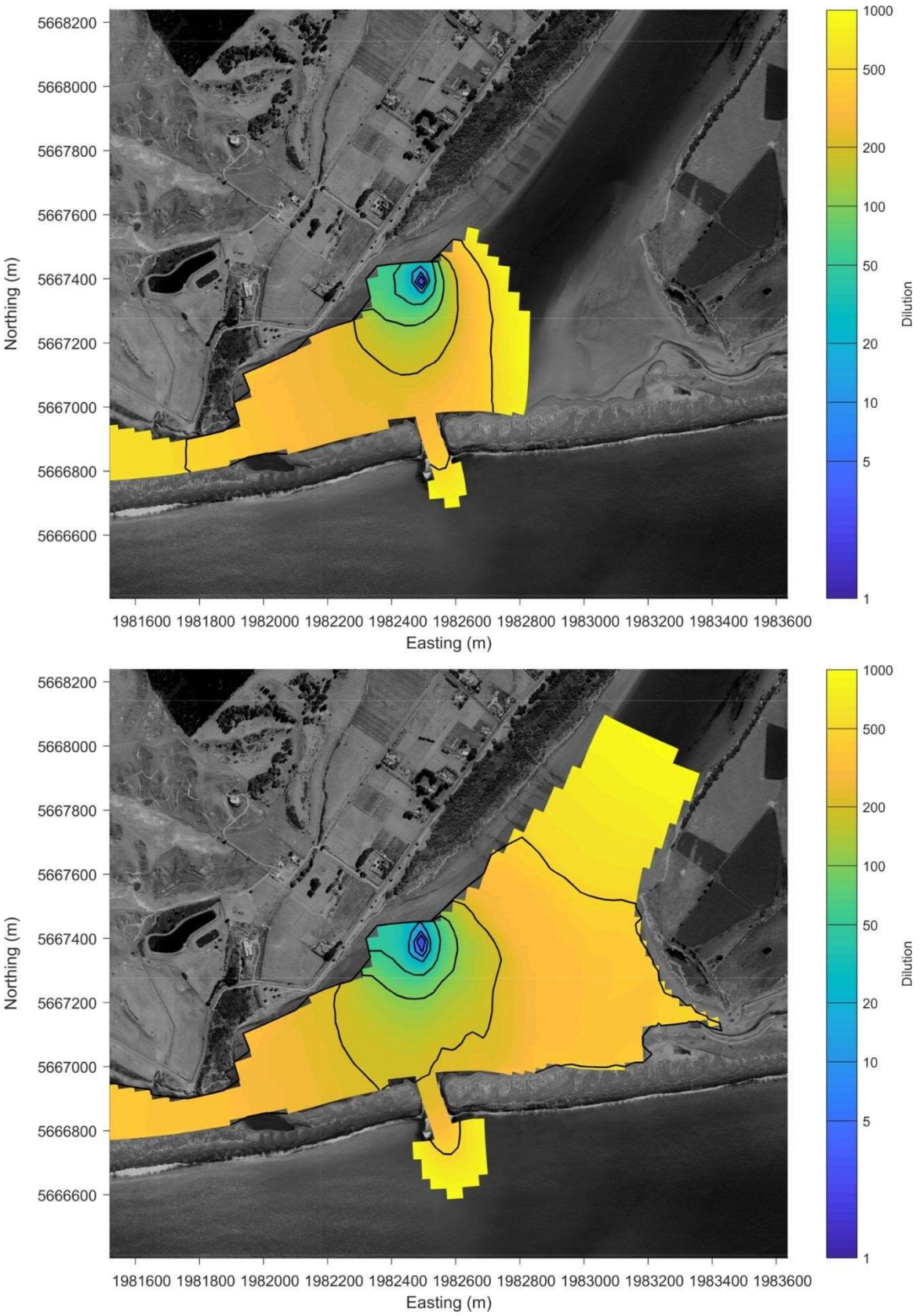

Figure 3.13. Dilution of the outfall for the calibration period. 95th (upper panel) and 99th (lower panel) percentiles.

3.6 Shear Stress

The seabed sediments are typically mobilised due to shear stress exerted on the seabed by moving water. Fine sediment usually mobilises when exposed to shear stress in excess of between 0.1 and 0.3 N m^{-2}. Shear stress can be calculated in the hydrodynamic model at each time step and can be used to identify areas that are expected to be highly mobile or where sediment is expected to accumulate. Hourly bed shear stress over a complete tidal cycle is shown in Figure 3.14 and Figure 3.15 illustrating high values near the mouth and reduced shear stress in the eastern and western arms.

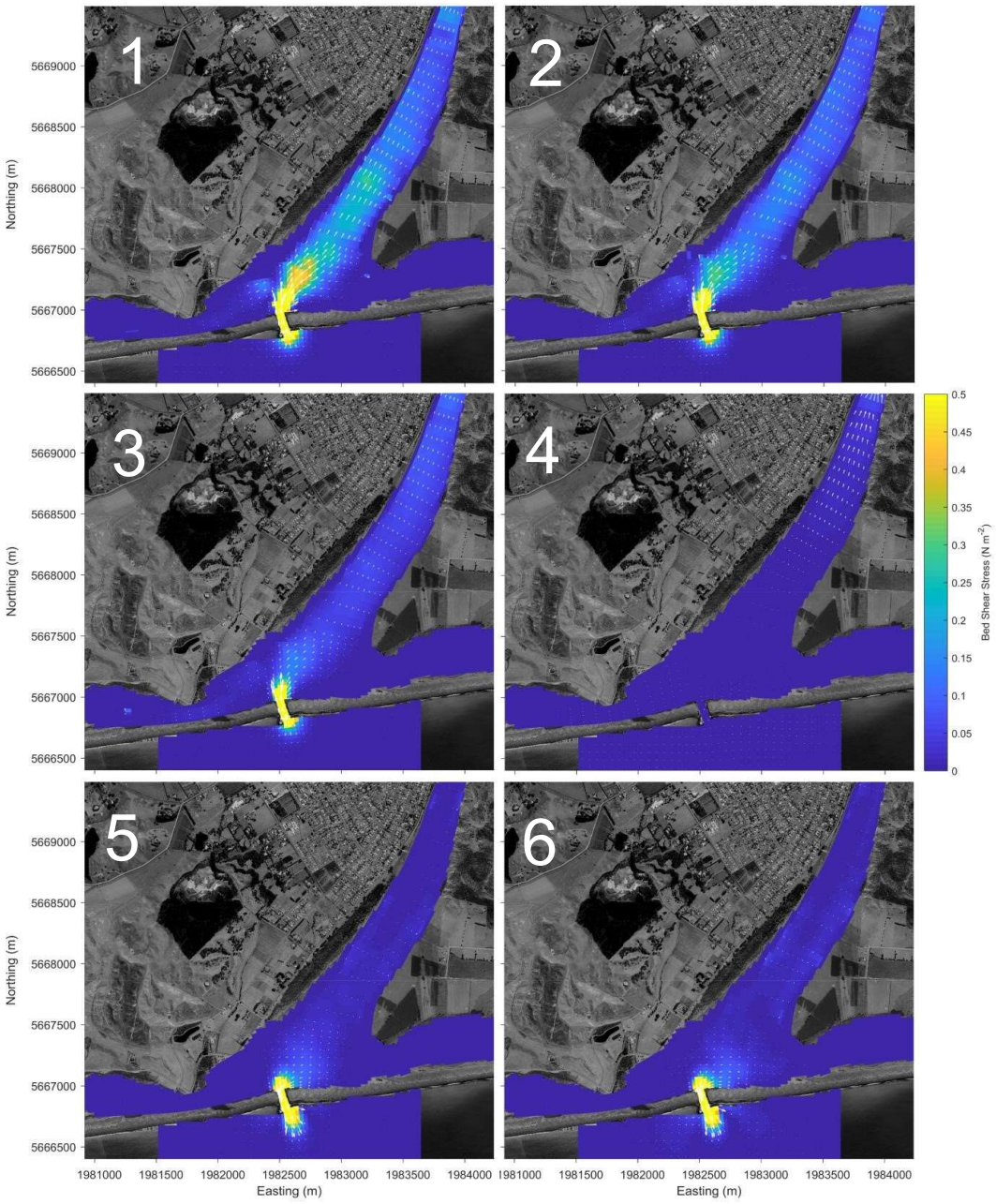

Figure 3.14. Modelled bed shear stress over hours 1 to 6 of a tidal cycle. The colour bar is capped at 0.5 N m^{-2}.

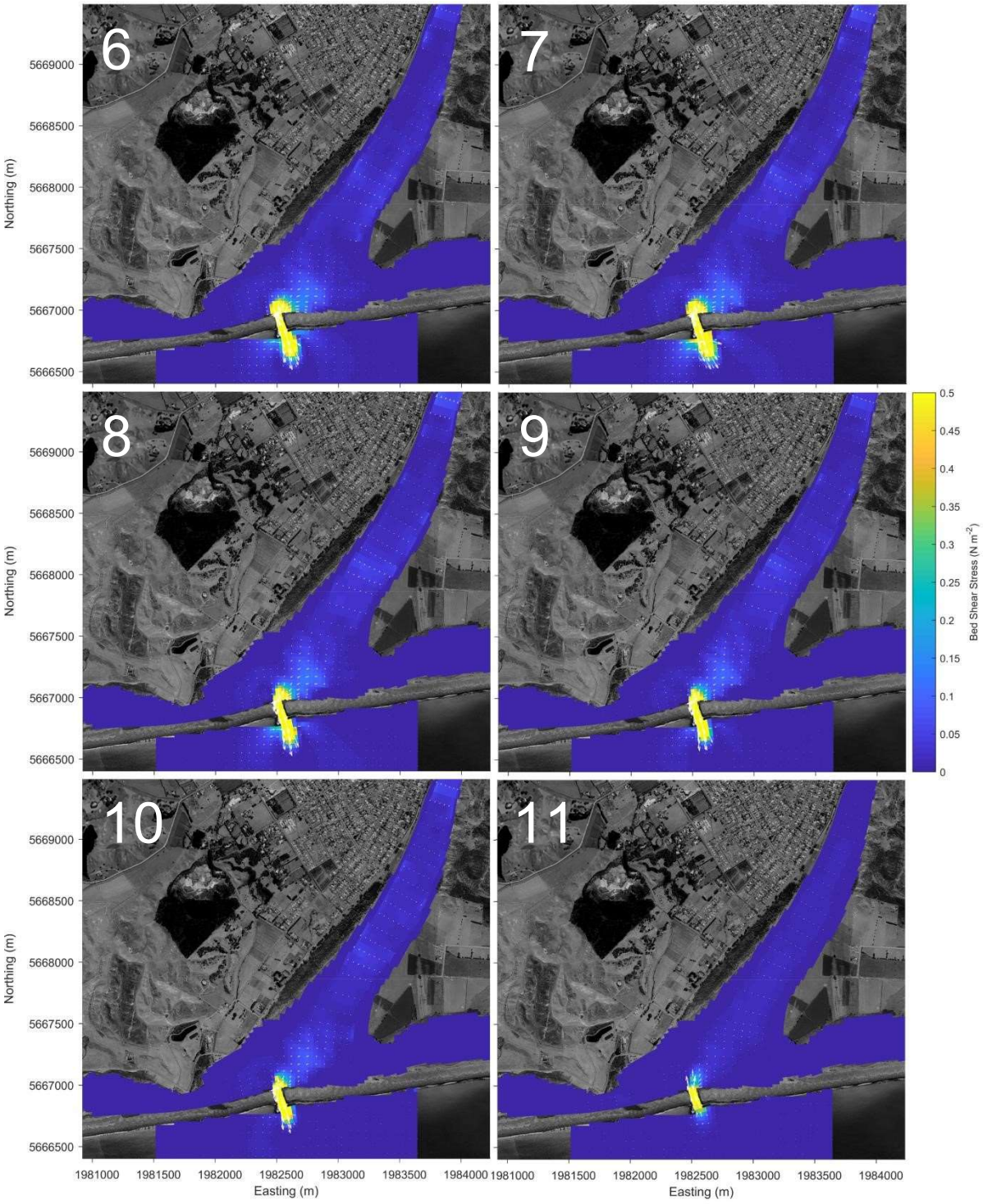

Figure 3.15. Modelled bed shear stress over hours 7 to 12 of a tidal cycle. The colour bar is capped at 0.5 N m^{-2}.

When the results of the sediment grain size analysis (Table 3.2) are compared to the modelled shear stress (Figure 3.14 and Figure 3.15), it can be seen that the samples with the highest percentage of fine sediment are located where the shear stress is lowest, and vice versa (see

Figure 2.2 for sample locations). For example, shear stress at Site G remains at or around zero throughout the tidal cycle and so is a deposition zone for fine sediments and has high silt content, while Site J experiences high shear stress throughout most of the tidal cycle and consequently has the lowest silt fraction (Table 3.2).

Table 3.2. 2018 silt/clay content results (<63µm). See Figure 2.2 for sample locations.

Site	Silt fraction (%)
A	68.54
B	19.26
C	64.45
D	32.57
E	61.82
F	59.13
G	80.47
H	87.23
I	36.1
J	13.88
Overflow	10.19

The anomalies to this include Sites B, H and the overflow. The overflow is in an area of low shear stress, however, this is the location of a small stream where fast flowing water runs through during rainfall removing fine sediments. Site H is on the edge of a high shear stress area, although the fine sediment content is some 87%. This is likely due to the exact configuration of the entrance during the surveys and how closely that has been replicated in the model domain (no current satellite image was available for digitizing); i.e. the site was just outside the area of higher shear stress at the time of sampling. Site B is interesting, since it is very close to other sites with high silt content, but has a relatively low percentage of fine material. Close inspection of model output indicates Site B experiences relatively higher shear stress than at Sites A and E due to an area of mostly low shear stress throughout the tidal cycle at the latter 2 sites (Figure 3.14 and Figure 3.15). Similarly, shear stress to the area southwest of the low zone at Sites A and E is increased resulting in a lower percentage of silt content at Site D (Figure 3.14 and Figure 3.15)

4 Discharge Modelling

4.1 WWTP outfall discharge simulations

4.1.1 Basis

The model was used to explore a range of scenarios under varying river and outfall flow conditions. Ten scenarios were run to represent potential future outfall discharge regimes, for which LEI had selected and developed specific criteria; these scenarios are described in Table 4.1. There were a number of iterations the led to the development of these scenarios. The first 8 scenarios feature discharge from the outfall only during out-going tides, whereas the final two feature continuous outfall discharge during high river flow.

Each model scenario was run for 12 days with 2 days used for model spin up and the remainder used to produce summary statistics.

Table 4.1: River and outfall flow scenarios

	River Flow	River flow (m^3/s)	Discharge Flow (m^3/d)	Timing of Discharge
Scenario 1	MALF	15	800	During out-going tides
Scenario 2	MALF	15	1,600	During out-going tides
Scenario 3	½ Median	30	1600	During out-going tides
Scenario 4	½ Median	30	2,400	During out-going tides
Scenario 5	Median	60	2,400	During out-going tides
Scenario 6	Median	60	3,200	During out-going tides
Scenario 7	2 x Median	120	4,000	During out-going tides
Scenario 8	2 x Median	120	6,000	During out-going tides
Scenario 9	3 x Median	180	6,000	Continuous 24hour
Scenario 10	3 x Median	180	10,000	Continuous 24hour

4.1.2 Results

The 10 scenario model runs are summarised here to compare spatial variability in dilution between the different runs. As with the calibration runs, 80th, 90th, 95th and 99th percentiles were calculated for each model grid cell for each model run after the spin up period. A transect was taken from the outfall along a line following the approximate ridge of lowest dilution towards the estuary mouth (Figure 4.1). The transect was extracted for each scenario and the results are shown in Figure 4.2 to Figure 4.6. Spatial maps of the 95th percentile dilution are shown in Figure 4.7 to Figure 4.11. As noted earlier, due to the initial dilution of the outfall in the release cell of the model, dilutions immediately next to the outfall should be treated with caution.

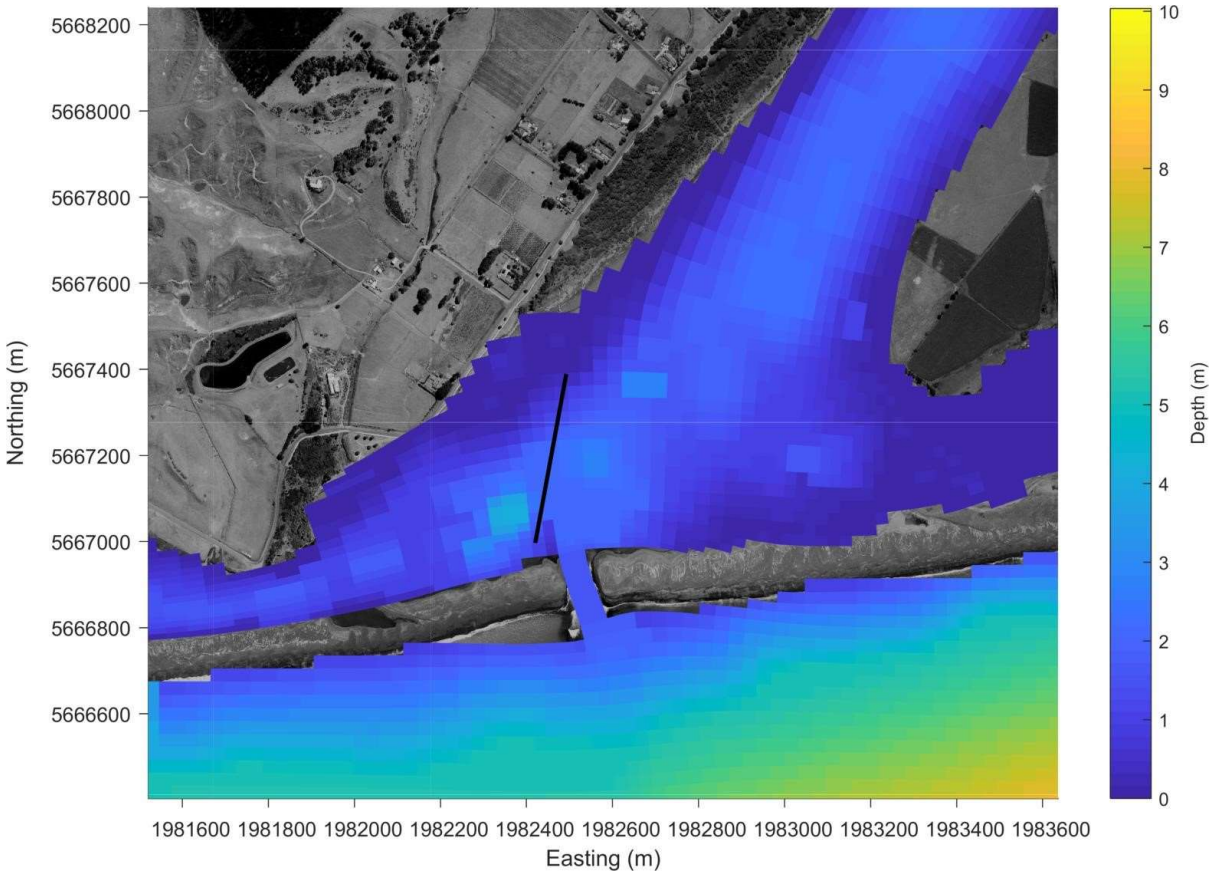

Figure 4.1. Dilution transect line used for subsequent transect dilution plots.

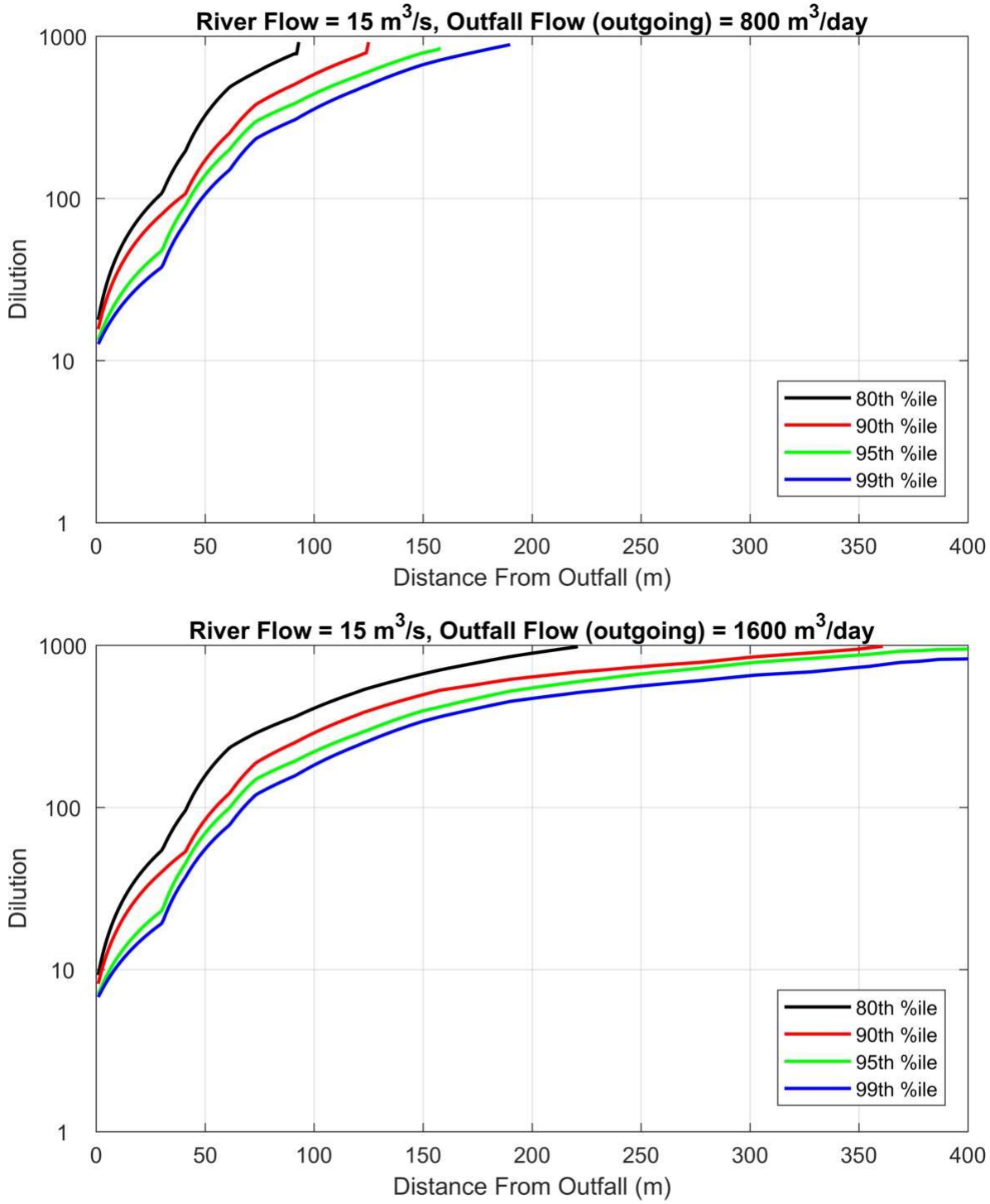

Figure 4.2. Scenario 1 (upper panel) and Scenario 2 (lower panel) dilution for a range of percentiles.

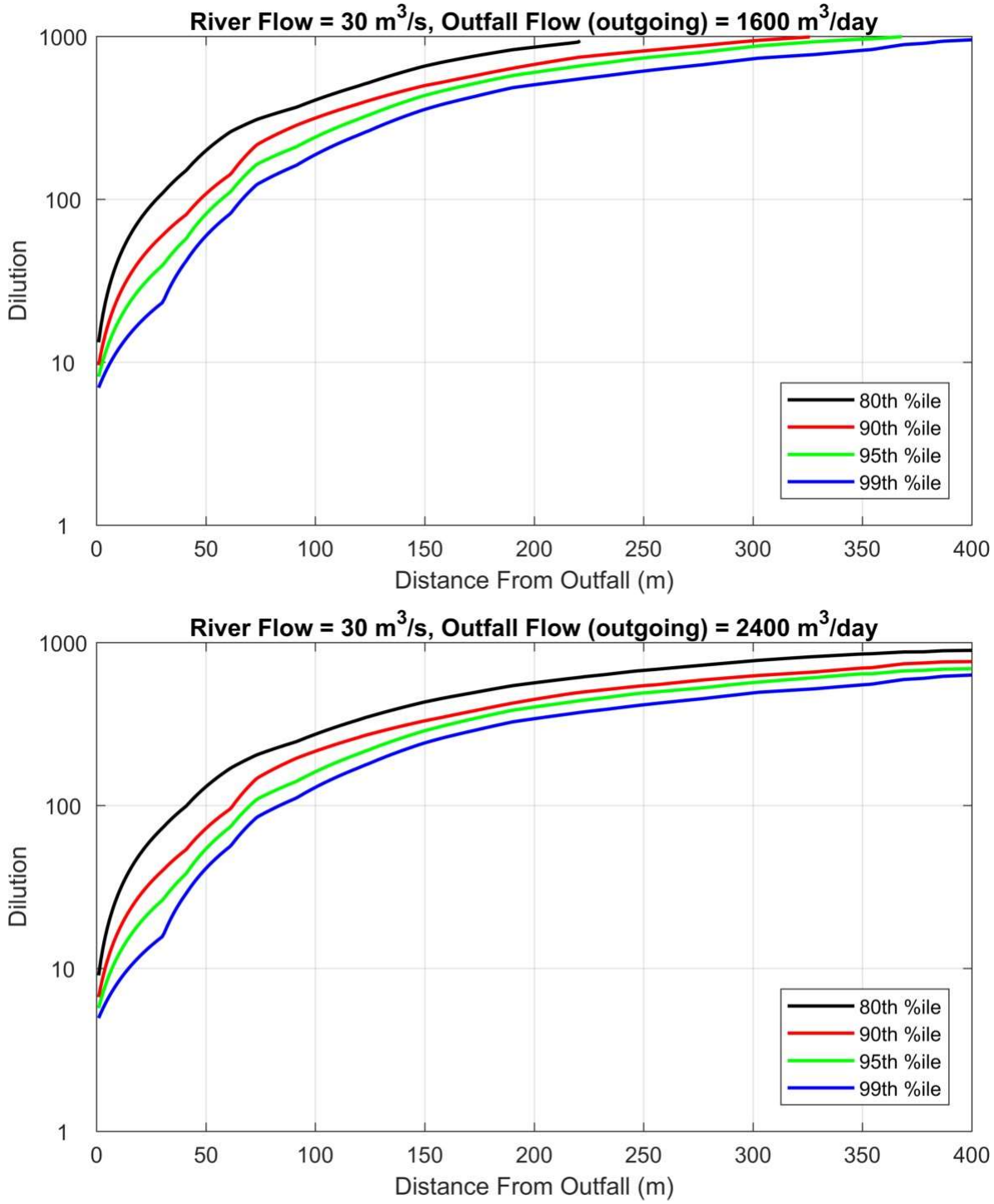

Figure 4.3. Scenario 3 (upper panel) and Scenario 4 (lower panel) dilution for a range of percentiles.

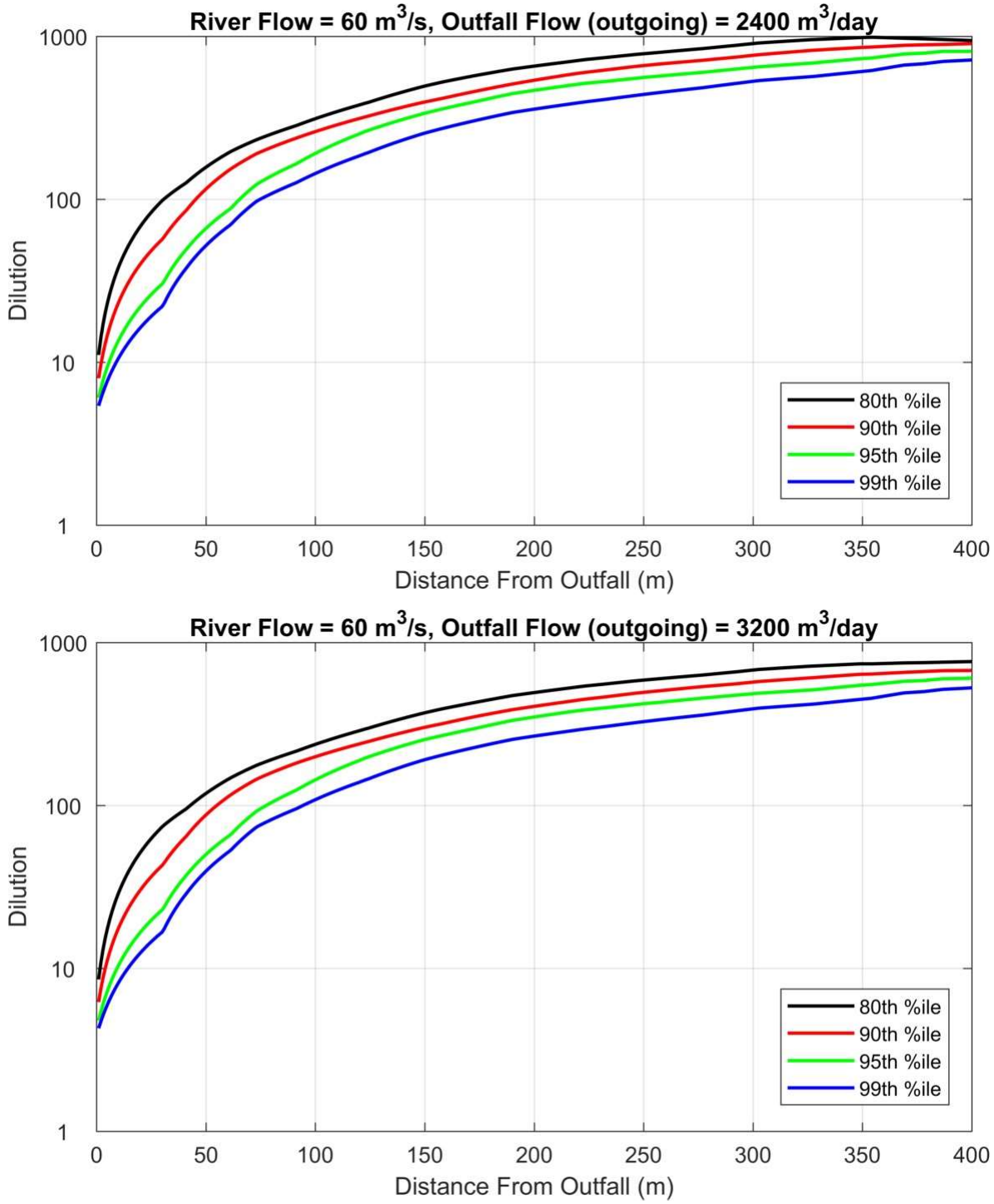

Figure 4.4. Scenario 5 (upper panel) and Scenario 6 (lower panel) dilution for a range of percentiles.

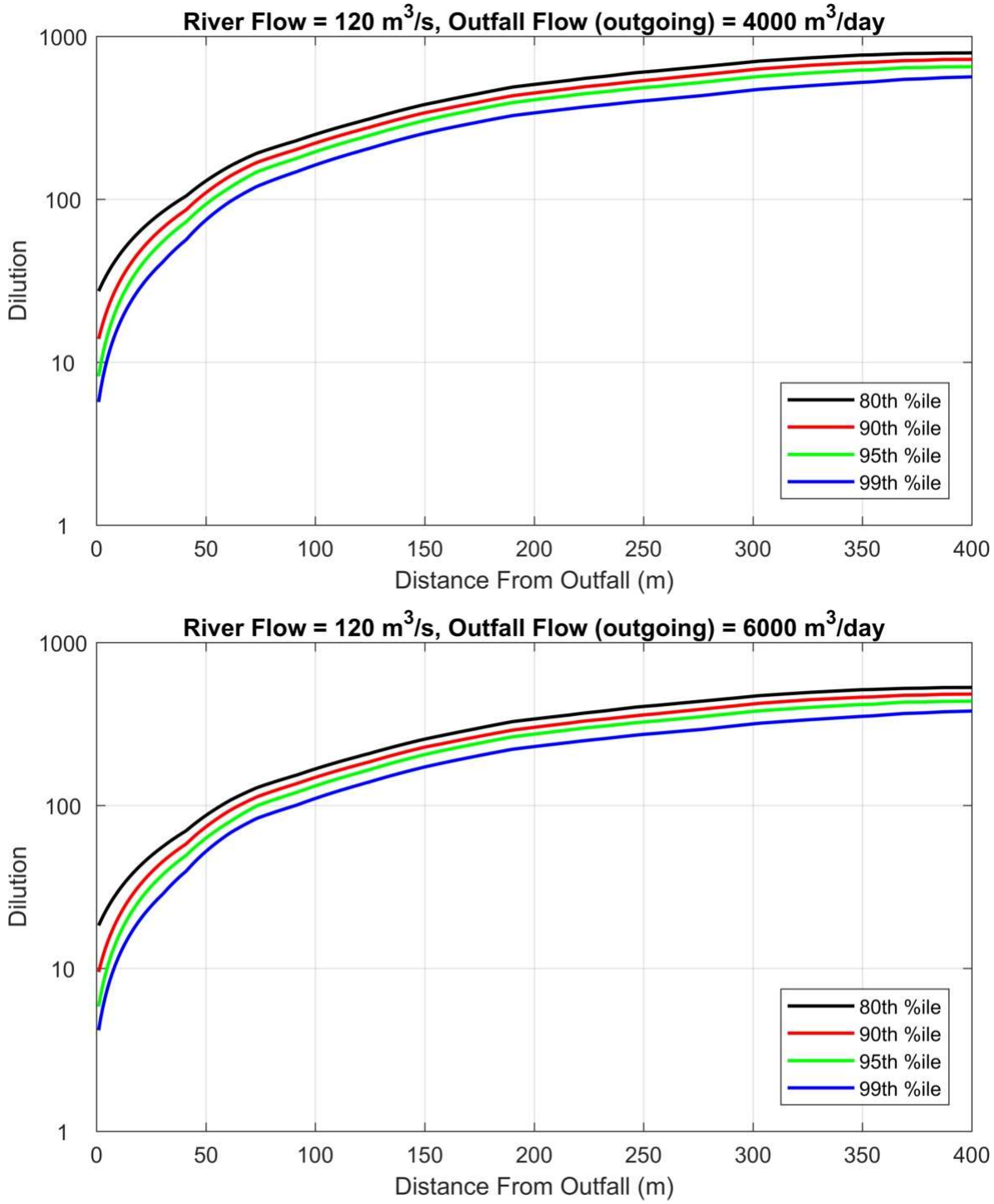

Figure 4.5. Scenario 7 (upper panel) and Scenario 8 (lower panel) dilution for a range of percentiles.

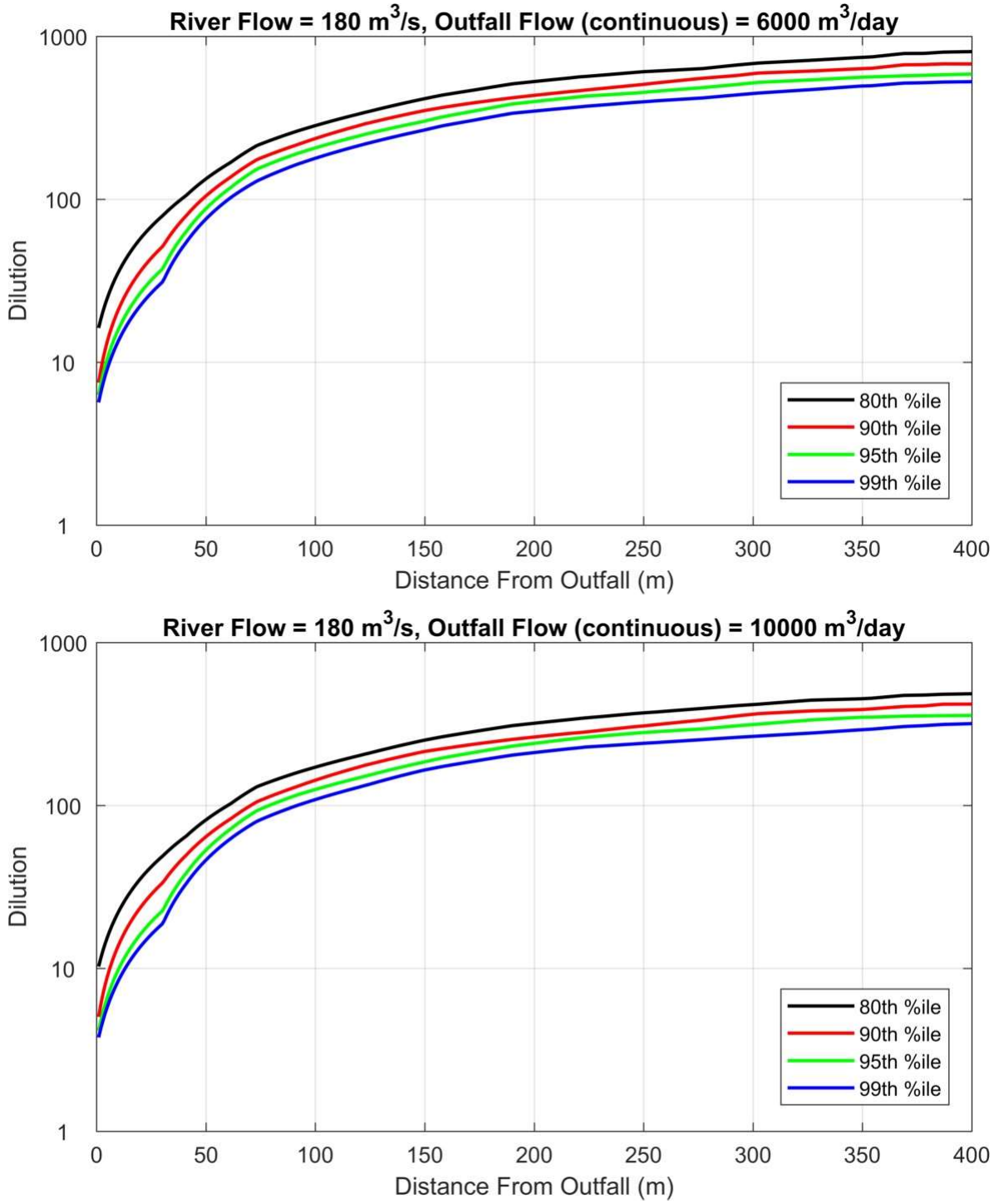

Figure 4.6. Scenario 9 (upper panel) and Scenario 10 (lower panel) dilution for a range of percentiles.

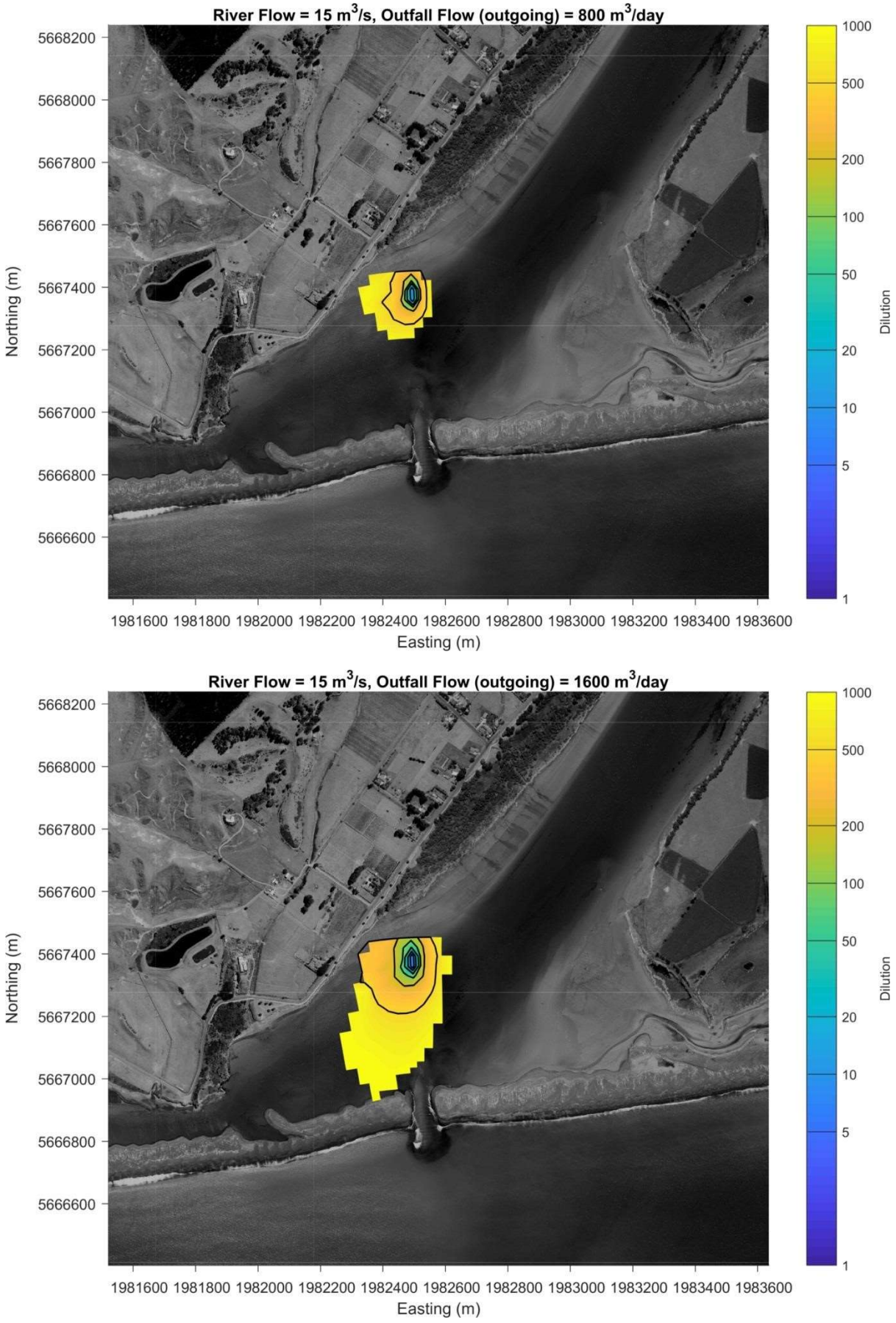

Figure 4.7. Scenario 1 (upper panel) and Scenario 2 (lower panel) 95th percentile dilution.

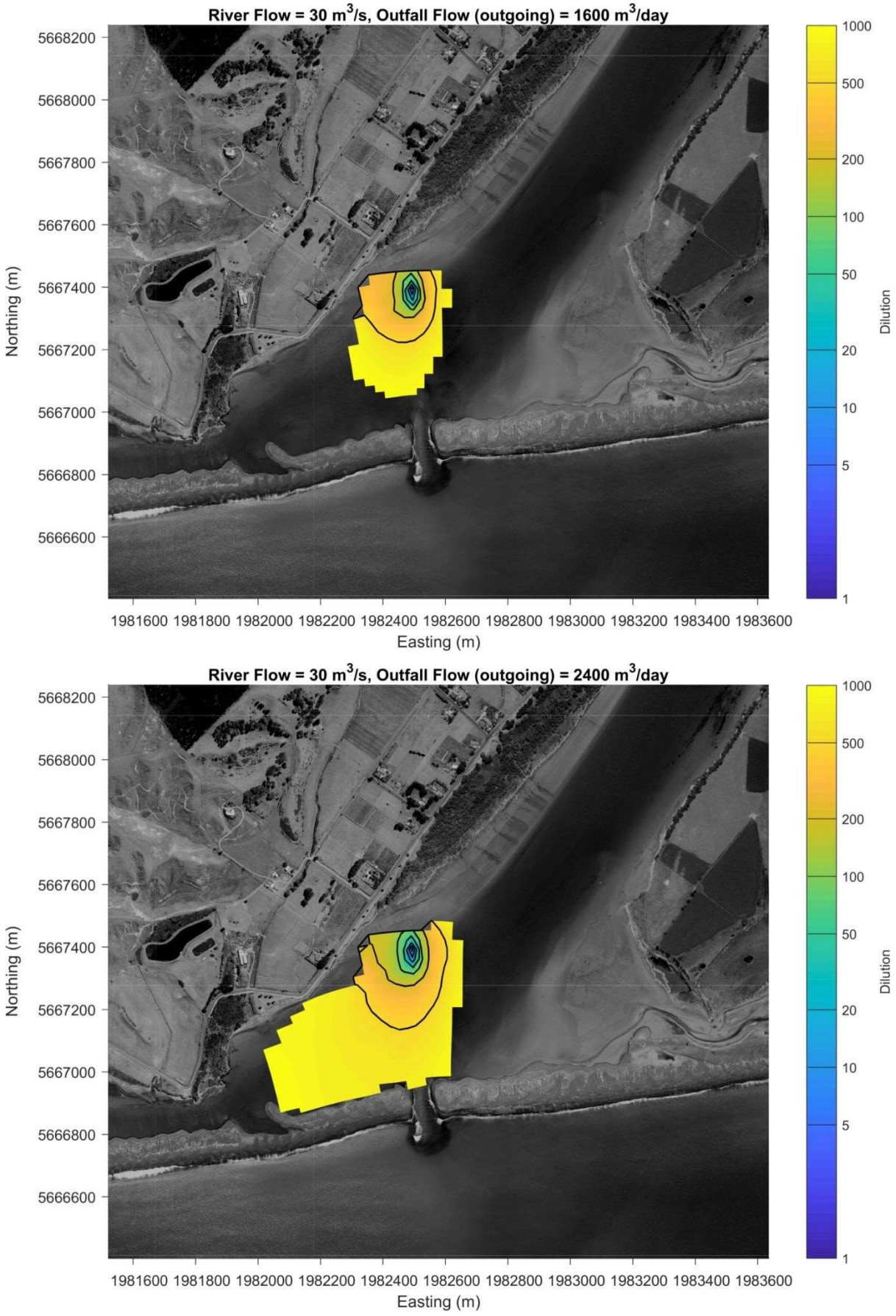

Figure 4.8. Scenario 3 (upper panel) and Scenario 4 (lower panel) 95th percentile dilution.

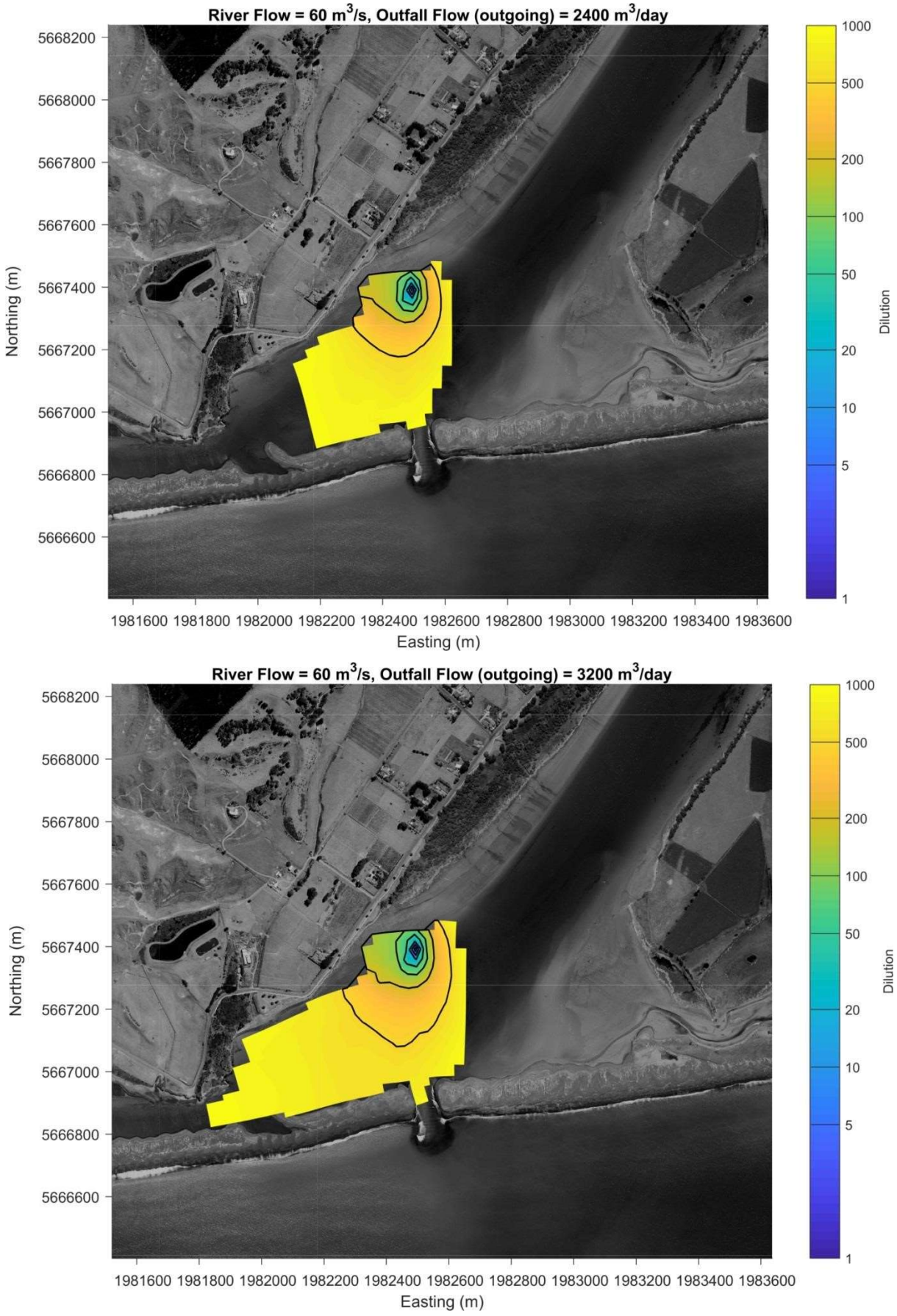

Figure 4.9. Scenario 5 (upper panel) and Scenario 6 (lower panel) 95th percentile dilution.

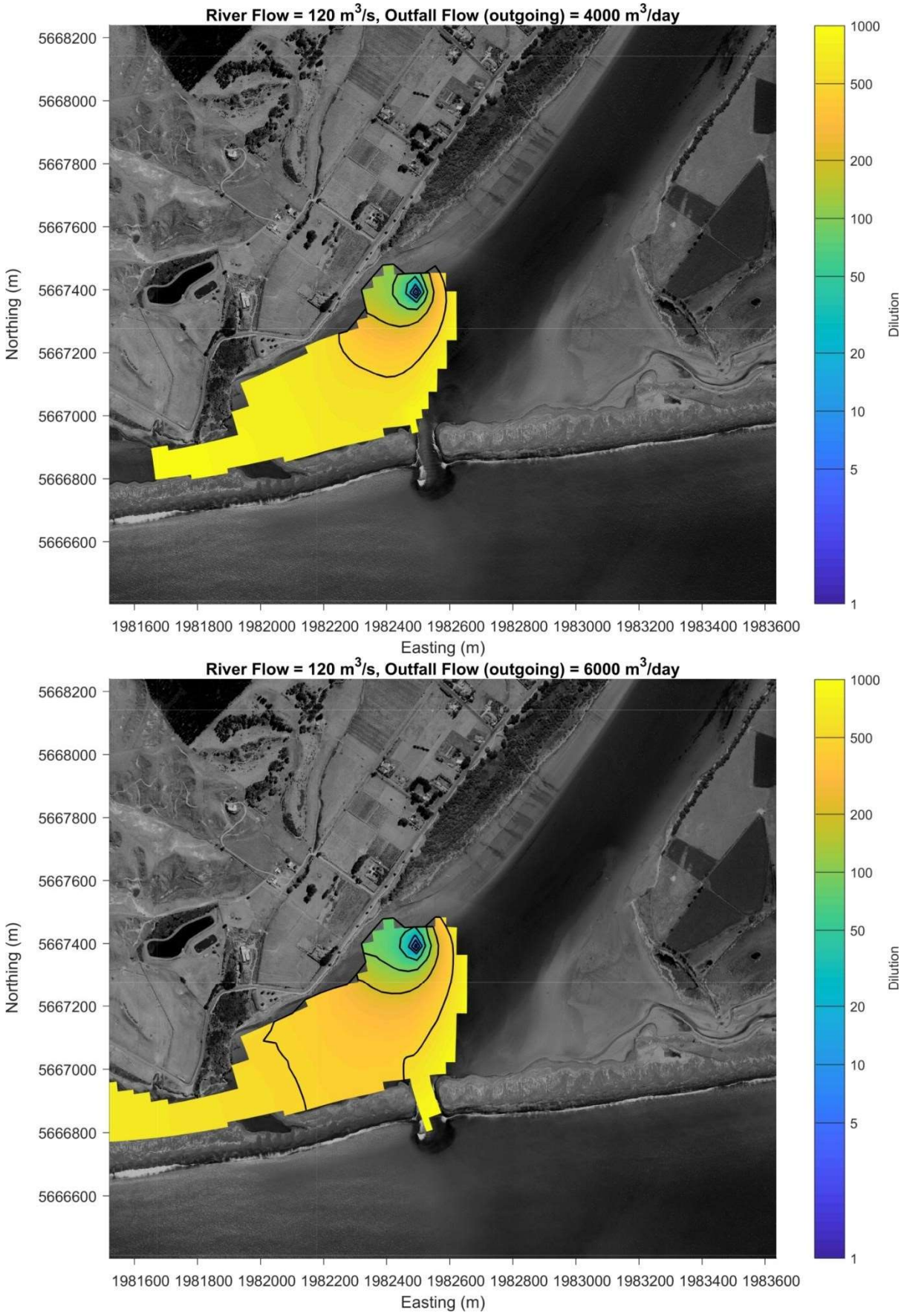

Figure 4.10. Scenario 7 (upper panel) and Scenario 8 (lower panel) 95th percentile dilution.

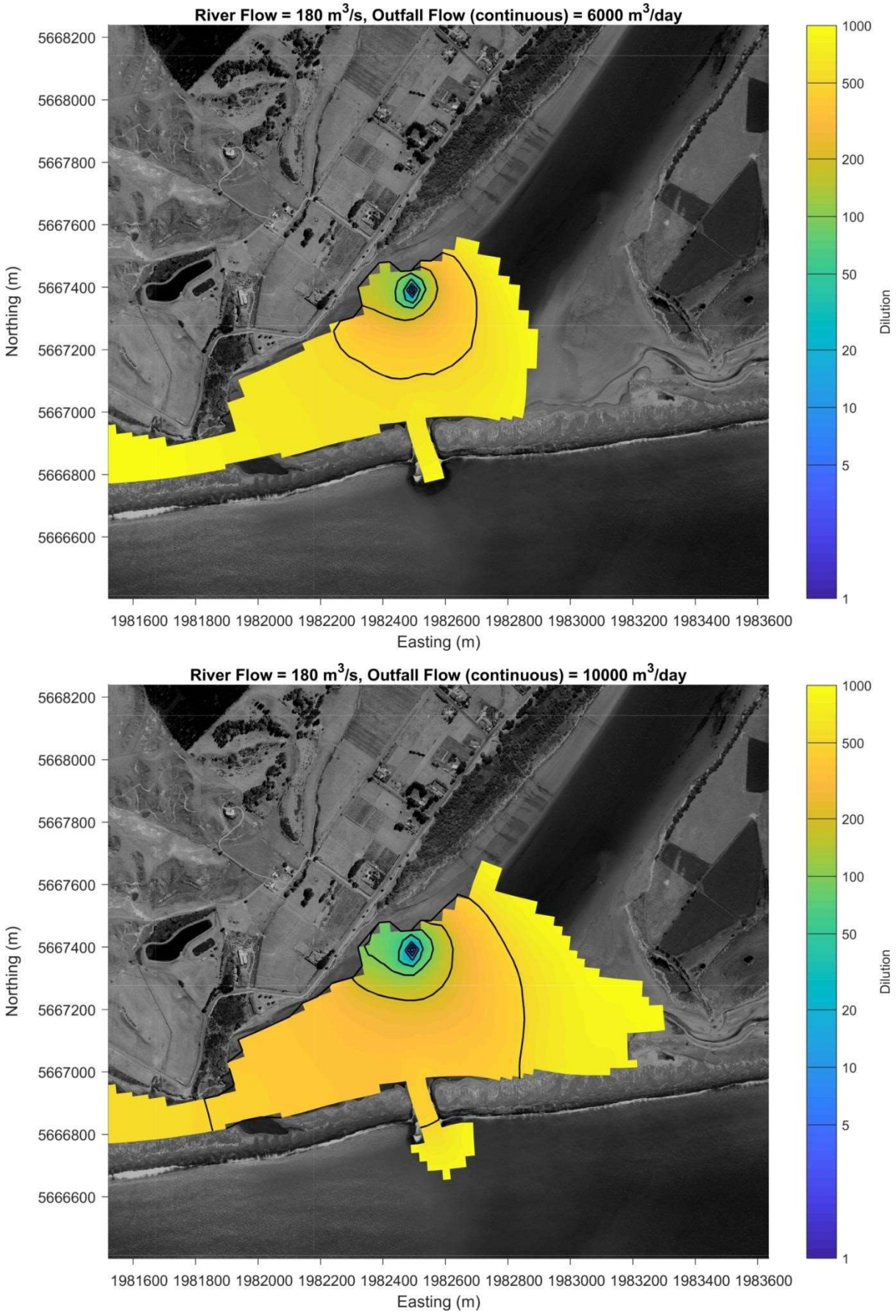

Figure 4.11. Scenario 9 (upper panel) and Scenario 10 (lower panel) 95th percentile dilution.

4.1.3 Discussion

In general, dilution increases with distance from the outfall, although the rate of dilution depends on both outfall flow rate and river flow. Increased river flow causes more rapid dilution of the outfall waters and increased outfall flow negates this effect. However, for these scenarios the area of the footprint of the outfall increases in scenarios with higher outfall flow. Scenarios 1 to 8 show lower dilutions towards the estuary mouth since discharge is only released on the outgoing tide.

For scenarios 9 and 10 discharge is released continuously, which results in lower dilutions also upstream from the outfall due to the incoming tide, despite the increased river flow. The dilutions upstream of the outfall are low and do not extend far north of the outfall because the in-coming tidal flows are reduced and often reversed at river flow rates of 3 x median (i.e., scenarios 9 and 10); that is the flows are high enough to negate the incoming tidal signal.

Analysis of the ~27 year record of river flow and river stage recorded at the railway bridge can help to give an indication of the amount of flow required to reverse the incoming tidal signal. The value is very variable as the required flow also depends on whether the tide is spring or neap. At times flows as low as 110 m^3/s can reverse the tide (during the smaller neap tides), although it seems like 250 m^3/s is a more usual value, although the tidal signal can sometimes be seen during flows upwards of 400 m^3/s (Figure 4.12). Therefore, there is a range of flow rates that can reverse the signal because the tidal elevation is different everyday, which is the predicted tide component; there are a whole suite of metocean factors such as barometric pressure, wind set-up, wave set-up, etc, that also contribute to varying the tidal elevation daily.

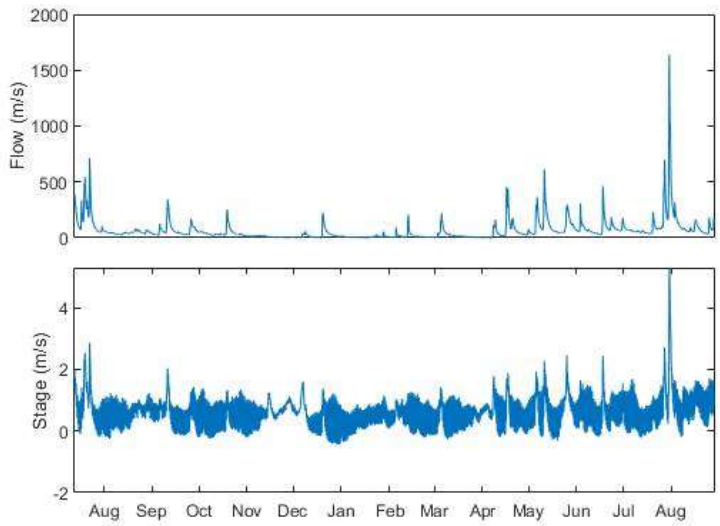

Figure 4.12. 13-months of river flow (top) and water level (bottom) data at the railway bridge over Wairoa River. Flows of 110 m^3/s can be seen to reverse the tide (small neap tides), although 250 m^3/s is a more usual value and the tidal signal can sometimes be seen during flows upwards of 400 m^3/s.

4.2 Pump station overflow discharge simulation

4.2.1 Basis

The characterisation of wastewater overflow issues occurring in the lower Wairoa River is discussed in depth in Opus (2012b) and LEI (2015). These documents form the basis of our understanding of timings, locations, quality and quantity of untreated sewerage entering the river through overflows. Note, the 19/20 March 2012 event (a 1 in 3-year event) was the only event available with flow data that could be used for model simulation, and even then, some assumptions were required and modelled flow data by Opus (2012b) had to be applied.

Observations and modelling by Opus (2012b) of a rain event over 19-20 March 2012 identified key locations of wastewater spills from the sewer network. This information is shown in Table 4.2 below. The four main overflow locations along with their contributions to the total spill volume during this event are highlighted in orange with their locations depicted in the image to the right.

This rainfall event was deemed to have an Annual Recurrence Interval (ARI) of 3 years (Opus, 2012b) with 126 mm of rain falling over a 30-hour period with peak intensities of up to 12 mm/hr. While the data gathered from this event shows a reasonable volume of spilt wastewater, it should be noted that it does not represent all overflow scenarios (locations and magnitudes) but rather gives an indication of the volumes expelled from these key locations in such an event.

Table 4.2. Overflow sites from the 19-20 March 2012 event with the major contributors highlighted in orange (source: Opus, 2012b). Image to the right displays the locations of the highlighted spills.

Catchment	Asset No	Type of Structure	Modelled Discharge Volume (m^3)	Location
North Clyde	SMN0700	Manhole	8	Ormond Road
	SMN0780	Manhole	14	Mackley Street
	SMN0650	Manhole	60	Crarer Street
	SMN0190	Manhole	19	Glengarry Place
	SMN0150	Manhole	1	Mahia Avenue
	SMN0010	Overflow Pipe	3,650	River Parade
Subtotal			**3,752**	
Alexandra Park	SMA0490	Manhole	63	Lockwood Place
	SMA0440	Manhole*	1,020	Marine Parade
Subtotal			**1,083**	
Kopu Road	SMK?	Manhole	5	Campbell Street
	SMK0284	Manhole	2,240	Kopu Road
	SMK0005	Overflow Pipe	6,500	Kopu Road
Subtotal			**8,745**	
Main Drain	SMF0380?	Manhole	1	Kitchener Street
Total			**13,581**	

Note: * While indicated as a manhole, and the fact that there is no Alex Park pump station overflow, the volume would suggest it is the pump station overflow.

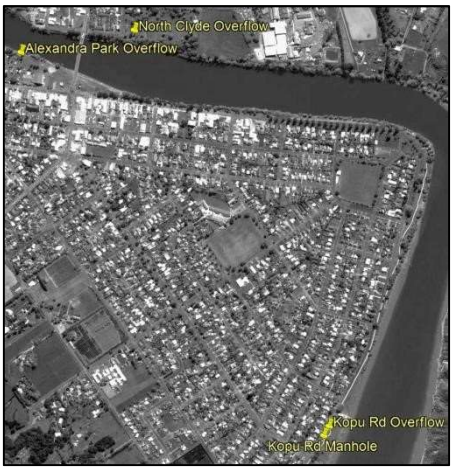

While there are eight other overflow points (manholes) tabulated, their combined spill volumes total 171 m^3, or just over 1% of the overall spill volume for this event. For the purpose of the hydrodynamic modelling, these minor overflow points were neglected.

Since overflow durations have not been measured, LEI (2015) analysed the Wairoa District Council's (WDC) sewer pump station wet-well level monitoring data for the period 2012-2014 (inclusive) in order to infer overflow durations from each pump station location during elevated wet well level periods. The data recorded for the 19-22 March 2012 event is shown in Table 4.3. These durations were applied to the point source overflows in the hydrodynamic model.

Table 4.3. Recorded overflow durations inferred from elevated wet well levels (source: LEI, 2015). 19-21 March 2012 event is highlighted in orange.

Date of Event	Total Daily Rainfall (mm)	Duration of Event (hh:mm)			
		North Clyde	Alexandra Park	Kopu Road	Fitzroy Street
1 January 2012	59.0	16:14	10:29	09:40	-
2 January 2012	6.8	-	-	00:59	-
8 January 2012	56.0	18:08	18:17	16:40	-
9 January 2012	1.2	00:30	01:30	02:50	-
19 March 2012	0.0	00:51	-	-	-
20 March 2012	82.2	24:00	22:30	20:26	-
21 March 2012	43.8	24:00	12:30	17:55	-
22 March 2012	1.2	00:30	-	-	-
4 April 2012	29.8	14:43	00:57	00:22	-
5 April 2012	25.0	10:10	-	-	-
8 May 2012	0.0	-	-	-	01:22
9 May 2012	5.4	-	-	-	02:15

Unfortunately, there are no records of sampled overflow water for contaminant analysis, so we can't be sure of the quality of the spills. However, EAM (2011) sampled 22 manhole sites throughout the sewer network and reported that conductivity was significantly reduced following a large rainfall event due to wastewater dilution from storm water ingress and groundwater infiltration. In addition, Opus (2012b) indicate that prior to a rainfall driven overflow event, significant periods of flushing occur throughout the network, and for a modelled overflow event at North Clyde occurring on the 1 May 2012, this amounted to 9 hours (see Figure 4.13). Opus estimated that the proportion of domestic sewerage in the overflowing water could have been less than 2%.

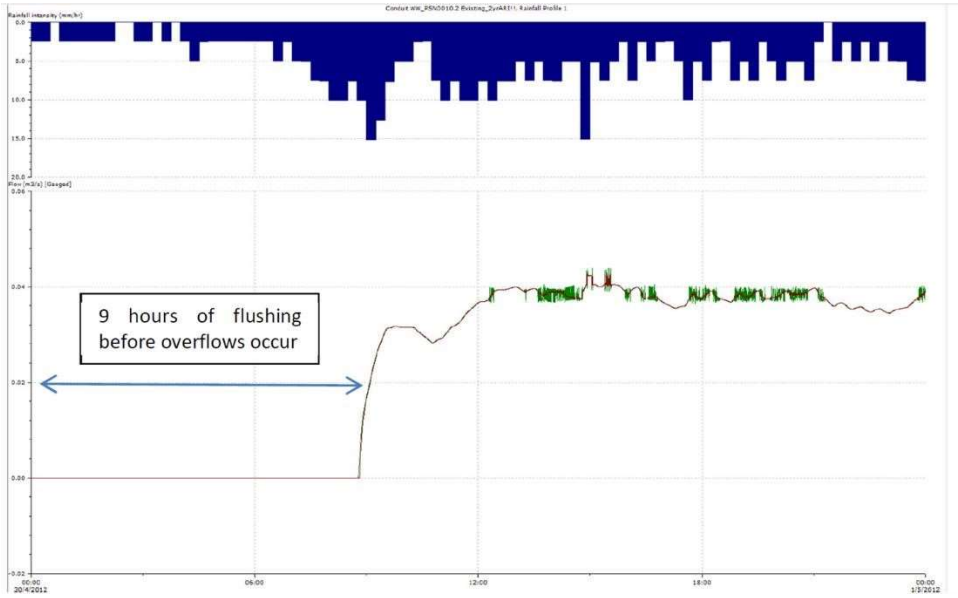

Figure 4.13. Modelled overflow hydrograph at the North Clyde pump station on 1 May 2012 (lower). Concomitant rainfall intensity is plotted also (upper). (Source from Opus, 2012b).

For the purposes of modelling, the two overflows at Kopu Road were combined into a single overflow since they were so close to one another spatially. Based on the flow record in Figure 4.13 flows were treated as being uniform throughout the spill period. A time series of the modelled flow during the spill event is shown in Figure 4.14.

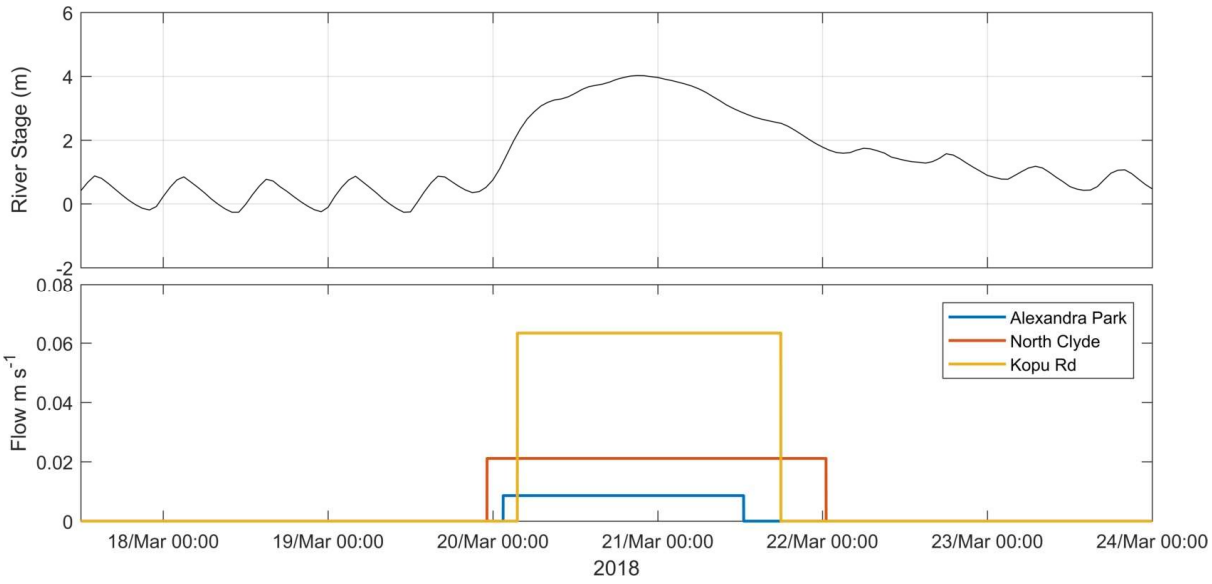

Figure 4.14. River stage and spill boundary conditions during the spill event of 19-22 March 2012.

4.2.2 Results

The spill event model run also used a conservative tracer to track the dilution of overflow water entering the receiving environment. As shown in Figure 4.15, the currents increased in the river due to elevated river level with almost 5 m s^{-1} currents occurring at the river mouth. As a result of the fast-flowing currents, the overflow water was diluted very quickly (see Figure 4.16) as it moved downstream with the river water. The highest concentrations of overflow water were seen at Kopu followed by North Clyde.

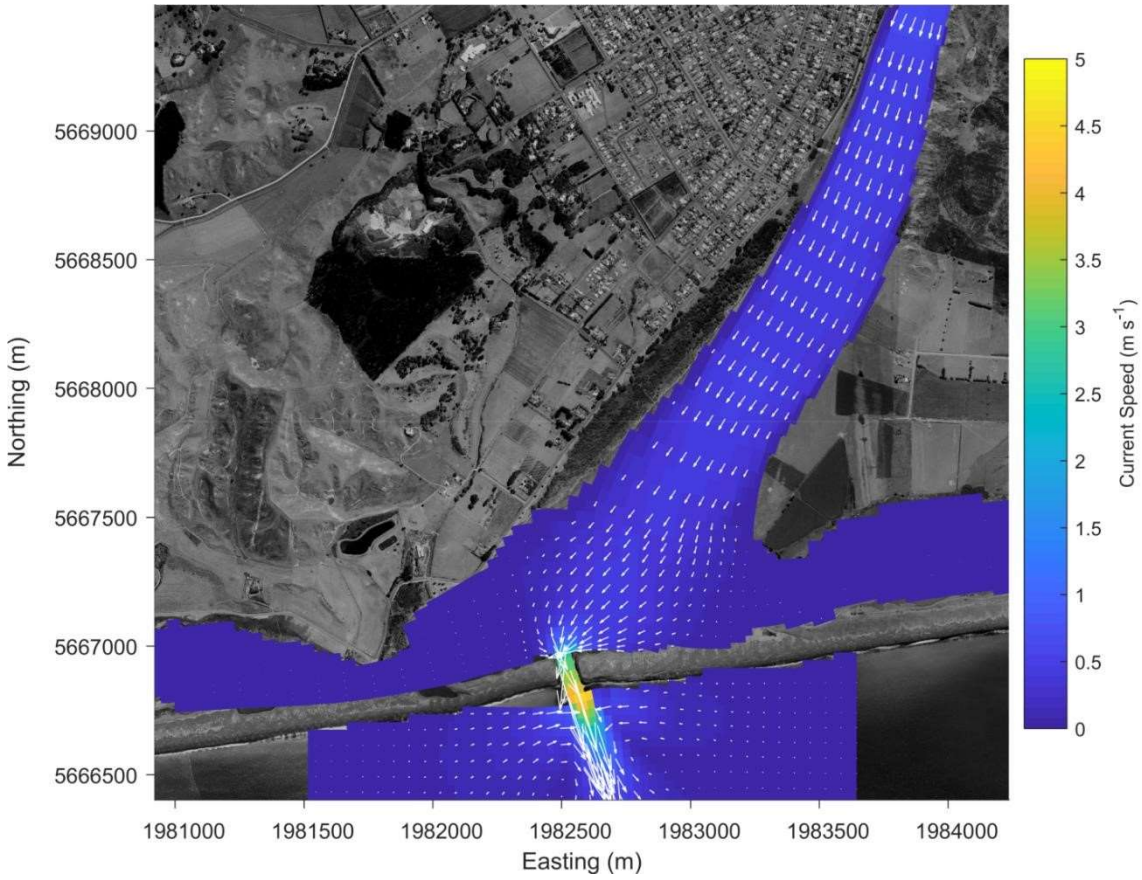

Figure 4.15. Peak flow due to elevated river stage during the spill event.

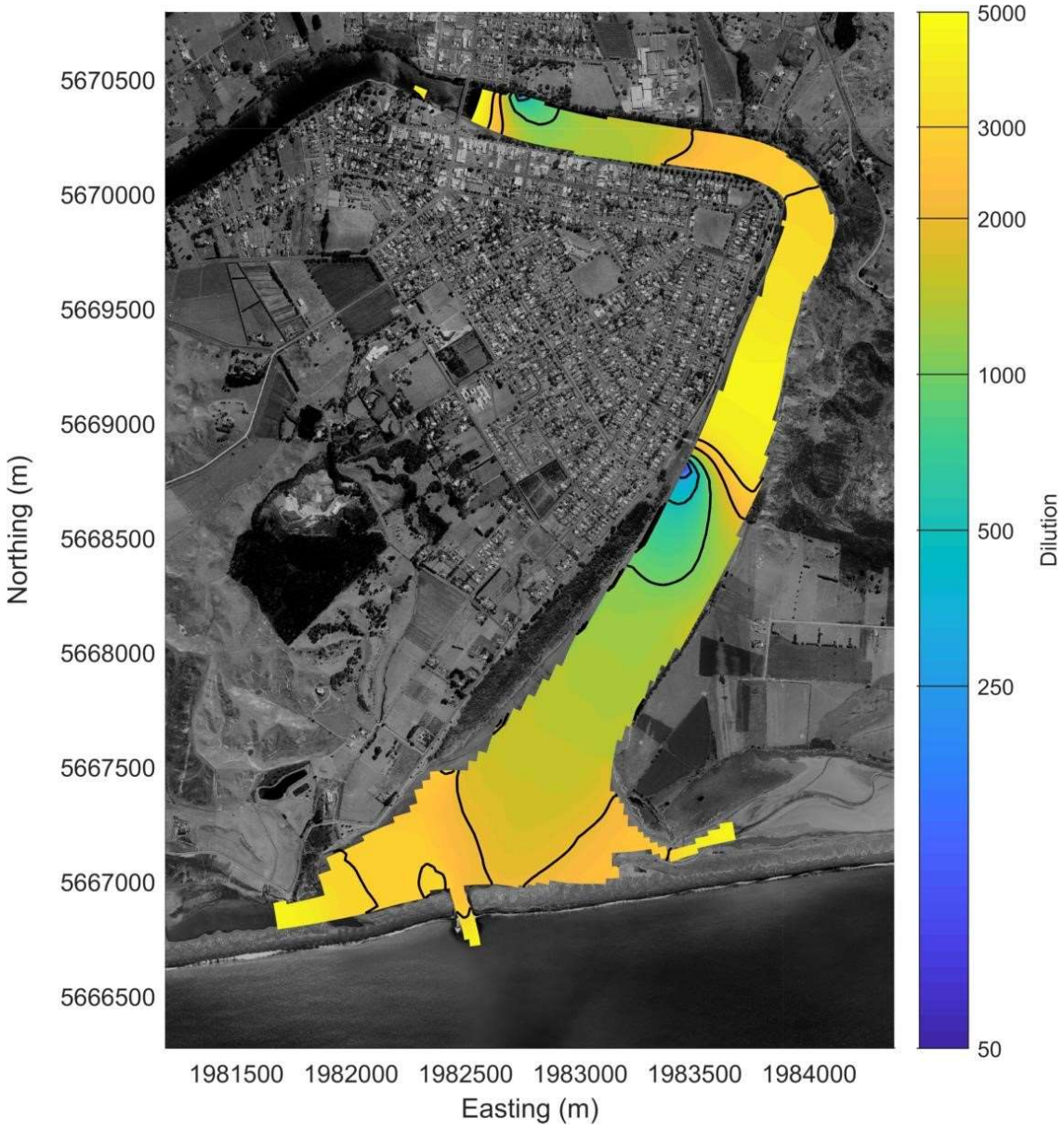

Figure 4.16. 99th percentile dilution of the spill for the 19-20 March 2012 rainfall event.

4.2.3 Discussion

During the March 2012 spill event peak river flow during this was 861 m^3 compared with the peak combined flow of the sewage that overflowed which was 0.09 m^3 or 0.01% of the peak river flow. Because of this disparity in flow, the spilled sewage was rapidly diluted into the ambient river water. The consequence of this is that while rain events can lead to overflows, they also create conditions where spilled substances can be rapidly diluted and flushed from the river by increased river flow.

5 Conclusions and Recommendations

A combined field data collection and 3D hydrodynamic numerical modelling project for the Wairoa River and the Wairoa WWTP discharge was successfully undertaken. The field data campaign included the successful collection of current, salinity, sea level and bathymetry data in the river mouth and the lower reaches of the river.

The model calibrated reasonably well against measured data in this hydrodynamically complex location, and replicated the important processes and degree of stratification identified in the measured data. This provides confidence in the results of the various modelled discharge and overflow scenarios modelled.

The model was used to explore the dilution of the wastewater spatially throughout the estuary for 10 scenarios with different configurations of outfall flow, timing and river flow developed by LEI to represent potential future outfall discharge regimes. Increased river flow causes more rapid dilution of the outfall waters and increased outfall flow negates this effect. However, for these scenarios the area of the footprint of the outfall increases in scenarios with higher outfall flow. Scenarios 1 to 8 show lower dilutions towards the estuary mouth since discharge is only released on the outgoing tide. For scenarios 9 and 10, where the discharge is released continuously, the outfall plume extends upstream due to the incoming tide.

An additional simulation was run to investigate the effects of a 3-year ARI rainfall event that resulted in a wastewater spill at 3 locations. Dilution maps showed the rapid mixing of the plume in the fast-flowing river associated with the rain event. This suggests that while rain events can lead to overflows, they also create conditions where spilled substances can be rapidly diluted and flushed from the river by increased river flow.

The morphology of the river mouth regularly changes over time and this will have some influence over hydrodynamics of the area which will in turn influence the pattern of dilution of the outfall.

The model has not been used to model specific contaminants (such as bacteria, nutrients, viruses and sediment) since monitoring data were not available to confidently generate boundary conditions and calibrate the model. However, the dilution maps and transect graphs can be used to provide a conservative estimate of pollutant concentrations from an assumed pollutant concentration at the outfall or overflow. As no pollutant concentrations have been used no attenuation or assessments of discharge effects on river water quality have been included in the modelling.

The results indicate that future ecological and sediment composition monitoring should include the western arm of the lower estuary, where outfall water is often retained, and shear stress is low.

References

Deltares, 2013. User Manual Delft3D-FLOW. version: 3.15.2789, May 2013 Published and printed by: Deltares, 706 p. available online: http://oss.deltares.nl/web/delft3d/manuals.

EAM (2011): Investigation of groundwater infiltration of the Wairoa District Council reticulated wastewater network. Unpublished report to Wairoa District Council, January 2011. 6 pp.

Egbert, G.D., and S.Y. Erofeeva, (2002), Efficient inverse modelling of barotropic ocean tides, J. Atmos. Oceanic Technol., 19(2), 183-204.

LEI (2015): Wairoa Wastewater Discharge Re-Consenting Summary of Wastewater and Stormwater Overflow Issues. Unpublished report to Wairoa District Council, October 2015. 50 pp.

Mead, S. T., T. Haggitt, W. Mead and S. O'Neill, 2018. Assessment of effects of Wairoa District Council's intertidal sewage discharge on benthic sediment characteristics and ecology – Wairoa Estuary. Report prepared for Wairoa District Council, June 2018.

Opus (2012b): Wairoa Wastewater Modelling – Stage 3 Detailed Wastewater Network Model. Unpublished report to Wairoa District Council, August 2012. 51 pp.